UNIVERSITAT POLITÈCNICA
DE
CATALUNYA

Experimental study and modelling of electrical arcs under high-voltage and low-pressure conditions for aerospace applications

---

Master's Thesis

Course: 2019-20

Master's Degree in Aeronautical Engineering

Author: **Rincón Ortiz, Juan David**

Director: **Riba Ruiz, Jordi Roger**

Co-Director: **Moreno Eguílaz, Juan Manuel**

Quisiera dedicar mi tesis a ...

Mi hermano, por ser un pilar imporante en mi vida ...

Mis padres que me han apoyado a lo largo de mis estudios y de mi vida ...

Y finalmente ...

Mi pareja por estar día a día respaldándome en todas las decisiones que he tomado.

Declaration of honour

I declare that, the work in this Master Thesis is completely my own work, no part of this Master Thesis is taken from other people's work without giving them credit, all references have been clearly cited, I am authorised to make use of the AMBER Laboratory related information I am providing in this document.

I understand that an infringement of this declaration leaves me subject to the foreseen disciplinary actions by The Universitat Politècnica de Catalunya – BarcelonaTECH.

Juan David RincÓn Ortiz		07/04/2020
Student Name	Signature	Date

Title of the thesis: Experimental study and modelling of electrical arcs under high-voltage and low-pressure conditions for aerospace applications.

Acknowledgements

First of all, I would like to thank God for the wisdom he has given me to finish this thesis and my studies as Aerospace Engineer.

I would like to express my special gratitude to Dr. Jordi-Roger Riba for imparting his knowledge and his expertise in this study. Also, for the help he has given me to obtain a research scholarship and be part of AMBER Laboratory.

Also, I would like to thank Dr. Álvaro for the support and help provided during the project. Thanks to his knowledge in electronics, I have been able to take results for my project.

It has been a pleasure and pride, to have been able to work on this project hand to hand with you Dr. Jordi and Dr. Álvaro, where I have been able to learn from a field that I had never explored and discover that it is a field that I am really passionate about.

Finally, I would like to thank all the people who have supported me throughout my life, who are my family. Also, to my friends who have shared beautiful moments with me during my academic life.

Resumen

Con el avance de la tecnología y específicamente en el sector aeronáutico, nuevos conceptos aparecen hoy en día como el llamado "More Electric Aircraft" que actualmente se ha podido ver con el último modelo de Boeing, el B787 o "Dreamliner", cuyo objetivo es crear un avión más eficiente en términos de peso y por ende se ve reflejado en la reducción de costes en combustible y en emisiones de CO2. Este concepto busca utilizar la potencia eléctrica para todos aquellos sistemas no propulsivos, como por ejemplo, en sistemas de control de vuelo o actuadores, y dejar de utilizar sistemas anticuados como son el hidráulico, el neumático y el mecánico para estos fines. Para ello, se requiere aumentar la potencia eléctrica generada por las fuentes, pero, este aumento en la demanda de potencia eléctrica y consecuente aumento de tensión, se puede ver perjudicado por las descargas parciales que se presentan en los cables o en los conectores de los aparatos electrónicos que conforman un sistema en el avión. En este trabajo, se estudiará el efecto corona en el cable aeronáutico "M22759-34" con una tensión nominal de 600 V donde se someterá a diferentes presiones desde los 10 kPa hasta los 100 kPa para encontrar la tensión a la que empiezan aparecer las descargas parciales. También, el estudio se hará bajo corriente eléctrica alterna, corriente continua con polaridad positiva y negativa para ver si el comportamiento del cable es diferente para las distintos tipos de corrientes que se pueda encontrar en el sistema eléctrico del avión. Se verá que la tensión de extinción no varía mucho según el tipo de corriente, pero sí según el "setup" que se utilice para realizar las pruebas. También, se probará tres tipos de detección para encontrar las descargas parciales, es decir, por detección visual , por antena y directamente midiendo la tensión en una resistencia en serie con el circuito. La detección por antena y por caída de tensión encuentran a la vez las descargas parciales mientras que la detección visual lo hace posteriormente. Análogamente, se estudiará el arco eléctrico bajo las mismas condiciones que en el caso del efecto corona.

Abstract

With the advancement of technology and specifically in the aeronautical sector, new concepts appear today such as the so-called "More Electric Aircraft" that has currently been seen with the latest Boeing model, the B787 or "Dreamliner", whose objective is to create a more efficient aircraft in terms of weight and therefore is reflected in the reduction of fuel costs and CO2 emissions. This concept seeks to use electrical power for all non-propulsive systems, such as in flight control systems or actuators, and to stop using outdated systems such as hydraulics, pneumatic and mechanic for these purposes. To do this, it is necessary to increase the power generated by the sources, but this increase in power demand can be affected by the partial discharges that occur in the cables or connectors of the electronic devices that make up a system in the airplane. In this work, the corona effect in the aeronautical cable “M22759-34” with a nominal voltage of 600 V will be studied, where it will be subjected to different pressures from 10 kPa to 100 kPa to find the voltage at which the partial discharges begin to appear. Also, the study will be done under alternating current, direct current with positive and negative polarity to see if the behavior of the cable is different for the different types of currents that can be found in the aircraft electrical system. It shall be seen that the extinction voltage does not vary much depending on the type of current, but it does depending on the “setup” used to carry out the tests. Also, three types of detection will be tested to find the partial discharges, that is, by visual detection, by antenna and directly by measuring the voltage drop in a resistance in series with the circuit. Antenna detection and voltage drop detection find partial discharges at the same time, while visual detection does so later. Similarly, the electric arc will be studied under the same conditions as in the case of the corona effect.

Table of contents

Page

Declaration of honour ii

Acknowledgements iii

Resumen iv

Abstract v

List of Figures viii

List of Tables x

1 Introduction 1

1.1 The More Electric Aircraft . . . 1

1.2 Objectives . . . 2

1.3 Report organization . . . 2

2 State of the art 3

2.1 Introduction . . . 3

2.2 Partial discharges . . . 3

2.2.1 Types . . . 4

2.2.2 Corona effect and electric arc . . . 6

2.2.3 Effect of pressure on partial discharges . . . 7

2.2.4 Consequences . . . 9

2.2.5 Prevention . . . 10

2.3 Regulations . . . 11

2.4 Methodologies . . . 11

2.4.1 Proposals . . . 12

2.4.2 Partial discharges detection . . . 20

2.5 Environmental impact . . . 21

2.6 Wiring materials for aerospace applications . . . 22

3 Experimental features **25**

3.1 Introduction . . . 25
3.2 Equipment and materials . . . 25
3.3 Electrical circuit . . . 27
3.4 Experimental set-up . . . 29
3.4.1 General set-up . . . 29
3.4.2 Corona detection set-up . . . 32
3.4.3 Electric arc detection set-up . . . 33
3.5 Experimental procedure . . . 33

4 Experimental results **36**

4.1 Introduction . . . 36
4.2 Sample 1: Spike-Plane method . . . 36
4.2.1 S1: Alternating current . . . 36
4.2.2 S1: Positive direct current . . . 39
4.2.3 S1: Negative direct current . . . 40
4.3 Sample 2: Cable coiled around a copper tube . . . 41
4.3.1 S2: Aternating current . . . 42
4.3.2 S2: Positive direct current . . . 43
4.3.3 S2: Negative direct current . . . 45
4.4 Sample 3: Cable coiled around a copper tube with defect on insulating coat . . . 47
4.5 Polarity effect: Comparative Positive and Negative DC . . . 48
4.6 Sample 4: Arc detection at 0.5 mm distance among electrodes . . . 49
4.7 Sample 5: Arc detection at 3 mm distance among electrodes . . . 51

5 Conclusions **53**

References **55**

Appendix **58**

List of Figures

1 More Electric Aircraft concept . . . 1
2 Conditions that wires are subjected from Intrusive Inspection done by AT-SRAC . . . 4
3 Internal partial discharges . . . 5
4 External partial discharges . . . 5
5 Nature of partial discharges . . . 6
6 Corona effect in a twisted wire . . . 6
7 Electric arc in a damaged twisted wire . . . 7
8 Altitude versus Pressure . . . 8
9 Paschen Curve . . . 8
10 Experimental Set-Up proposed by Josef Hanson and Dieter Koenig. . . . 12
11 Cables disposition . . . 13
12 Measurement setup proposed by Benjamin Cella . . . 13
13 Twisted pair of enameled wires. . . . 14
14 Experimental Set-Up proposed by El Bayda et al. . . . 14
15 Experimental Set-Up proposed by T. André et al. for LF. . . . 15
16 Experimental Set-Up proposed by T. André et al. for HF. . . . 16
17 Experimental Set-Up proposed by T. André et al . . . 17
18 Sample proposed by Rui et al. . . . 18
19 Experimental Set-Up proposed by Rui et al. . . . 18
20 Experimental Set-Up proposed by Mermigkas et al. . . . 19
21 PVC/Nylon fire ignition study . . . 23
22 Electrical and RF detection of partial discharges. . . . 27
23 AC configuration. . . . 28
24 Positive DC configuration. . . . 28
25 Negative DC configuration. . . . 29
26 Source and vacuum chamber . . . 30
27 Structure for visual detection . . . 31
28 Top of the lid: antenna and metal rod. . . . 31
29 Corona detection setups. . . . 32
30 Arc detection setup. . . . 33

31 Experimental procedure flowchart. 34
32 Spike-Plane test under alternating current. 36
33 Visual and radio-frequency/electrical detection of spike-plane test. 38
34 Spike-Plane test under positive direct current. 39
35 Spike-plane visual detection: DC+. 40
36 Spike-Plane test under negative direct current. 40
37 Spike-plane visual detection: DC-. 41
38 M22759/34 sample test without defect under alternating current. 42
39 Visual and radio-frequency/electrical detection under AC current. 43
40 M22759/34 sample test without defect under positive direct current. 44
41 Visual and radio-frequency/electrical detection under DC current. 45
42 M22759/34 sample test without defect under negative direct current. 45
43 Sample 3 test under alternating current. 47
44 Visual detection on sample 3. 48
45 Breakdown voltage and current for a gap of $d = 0.5$ mm. 49
46 Arcing visual detection for a gap of $d = 0.5$ mm. 51
47 Breakdown voltage and current for a gap of $d = 3$ mm. 51
48 Arcing visual detection for a gap of $d = 3$ mm. 52

List of Tables

1 Features of each proposal. 20
2 Aircraft wiring 22
3 Sample 1: AC results for visual and antenna detection. 37
4 Sample 1: DC+ results for visual and antenna detection. 39
5 Sample 1: DC- results for visual and antenna detection. 41
6 Sample 2: AC results for visual and antenna detection. 42
7 Sample 2: DC+ results for visual and antenna detection. 44
8 Sample 2: DC- results for visual and antenna detection. 46
9 Sample 3: AC results for visual and antenna detection. 47
10 Sample 4: AC, DC+ and DC- results for arcing detection (d = 0.5 mm). . . 50
11 Sample 5: AC, DC+ and DC- results for arcing detection (d = 3 mm). . . . 52

1 Introduction

The growth of air transport is one of the biggest challenges that the aeronautical sector has to face in the coming years. This growth involves many problems that are affecting the melting of the poles in the Arctic and Antarctica due to the climate change that our planet is suffering. The environmental impact of flying an aircraft is very high since the gases emitted by the aircraft contribute greatly to the greenhouse effect and, therefore, giving way to global warming which is the main cause of climate change.

1.1 The More Electric Aircraft

Nowadays, with the advancement of technology, the aeronautical sector has been studying new concepts and creating different alternatives to reduce such environmental impact. Among these alternatives exists the creation of an aircraft capable of flying through the use of hydrogen as fuel and, the latest, the concept of MEA (the More Electric Aircraft).

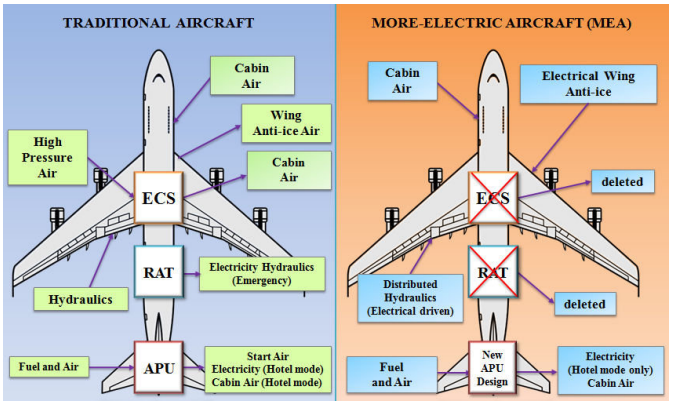

Figure 1: More Electric Aircraft concept. Source: [1]

Generally, aircraft components that are not propulsive, are controlled by different energy sources that come from the hydraulic, pneumatic and electrical system. The MEA concept offers to replace those components that have as a source the pneumatic and hydraulic systems and recreate them so that they can be operated by the electrical system. In this way, optimize the aircraft so that operating and maintenance costs are reduced, in addition, the emissions would also be reduced as there would be greater energy efficiency. The More Electric Aircraft is leading to a growing demand in power needs. Consequently, increasing power denotes either increasing the voltage supplied by the power source or increasing the maximum current that can be released from the source. In order to tolerate

this high current and high voltage, the cables shall resist and be highly reliable, and this is possible if the diameter of the cable is also increased. However, the wires can be damaged because of the mechanical stresses that are subjected during operation. Generally, in aircrafts, damages on wires, pressure and high voltage favours to have the phenomenon of partial discharges (among other aspects that contributes to the appearance of partial discharges).

1.2 Objectives

The objectives of the project are the following:

- Study the corona effect in aeronautical wires for different pressures that shall simulate the altitude at which the aircraft is flying.
- Identify the inception voltage with the aim of avoiding arc faults that can produce heat, break down the wire's insulation and trigger an electrical fire.
- Involve in the study, DC and AC circuits, to see which is the behaviour of the wires under both type of currents.
- Identify the breakdown voltage at which the arc appears for different pressures. It is wanted to make the experiments from 10 kPa to 100 kPa that is the atmospheric pressure at sea level.

1.3 Report organization

This document is organized into the following chapters:

- **Chapter 2: State of the art.** This chapter gives the basics of electricity and electronics to allow the reader to understand the physics of the project.
- **Chapter 3: Experimental features.** This chapter details which is the equipment and the setup used to execute the experiments and also describes the procedure followed to get the results.
- **Chapter 4: Experimental results.** This chapter exposes the main results of the measurements.
- **Chapter 5: Conclusions.** This chapter brings the conclusions of the results from the previous chapter which are gathered and analyzed.

2 State of the art

2.1 Introduction

The project is totally related to partial discharges (PDs) field. Therefore, this part shall provide the basic knowledge involving partial discharges, regulations to detect and avoid this important phenomena and expose which are the common methodologies that are used in experiments to advance the appearance of partial discharges. Also, it is important to raise awareness about the impact than can generate PDs to security, in this case in aircrafts, and also to the environment. Finally, it is made an historical background of the materials used in the aerospace sector for wiring and it is listed at the end of this section which are the common insulation materials nowadays.

2.2 Partial discharges

Partial discharges occur when the breakdown field strength of the dielectric is locally exceeded due to varying local field intensity or varying local voltage resistance, resulting in the partial breakdown of the insulation system. To start partial discharging, the voltage must lie above the level of the relevant PD inception voltage V_{PDIV} [2]. This phenomenon is a consequence of arc tracking where a plastic material is transformed from non-conductive to conductive through a process of surface degradation.

The occurrence of the phenomenon depends on factors such as temperature, pressure, humidity, insulation type and thickness, voltage magnitude and waveform applied between the electrodes [3]. The degradation of the insulation material is advanced by aging factors such as stressors at which the wires are subjected during aircraft's life. In [4], the Aging Transport Systems Rulemaking Advisory Committee (ATSRAC) documented the presence of wire deterioration in different zones of aged aircraft. It was not possible to determine quantitatively the aging of the wires due to an original wire of the same age was not available for a direct comparison to understand the deterioration of the wire's physical characteristics, but it was possible to report the main conditions of wires from various examined aircrafts. These conditions allowed to define some of the stressors that are present in the aircraft.

Heat, vibration and chemical contamination are common stressors in aircraft's wiring depending on the position is used, also there are other conditions that are a consequence of the previous stressors as the cracked and abraded insulation. In Figure 21, it is possible to identify the conditions of the wires in an aircraft.

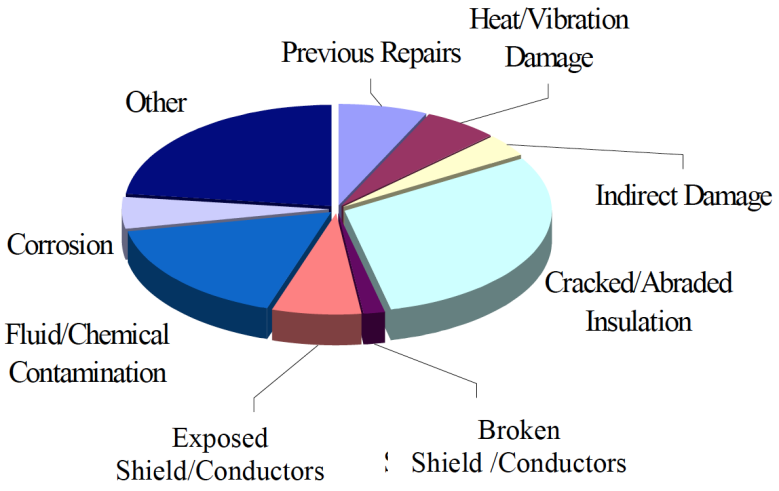

Figure 2: Conditions that wires are subjected from Intrusive Inspection done by ATSRAC. Source: [4]

2.2.1 Types

Depending on the defects that the wiring insulation material has, it is possible to differentiate two types of partial discharges. These are the internal and external partial discharges [3].

- **Internal defect**:

  The internal discharges are usually due to cavities within the electrical insulation. The cavities are weak points inside the insulator and are normally produced by bad manufacturing or due to aging of the material. The electric field within a cavity is equal to or greater than the electric field surrounding the insulation. This is because the gas has a lower dielectric strength than the surrounding insulation and as a result, the cavities are weak points within the insulation, where the PD activity begins.

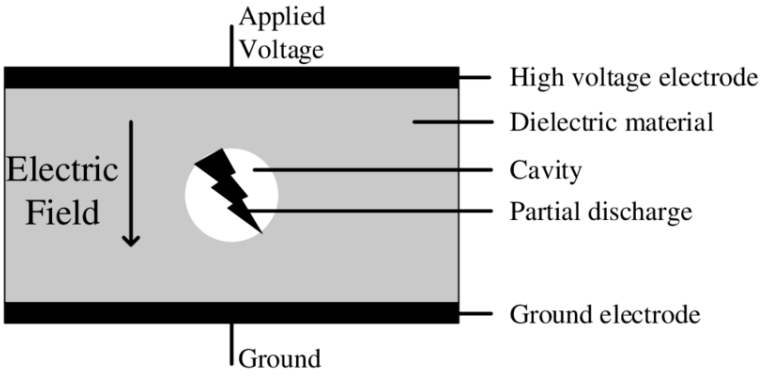

Figure 3: Internal partial discharges. Source: [5]

- **External defect**:

  The external defect, or surface defect, depends mostly on the physical shape of the component. An external space can be the location of intense discharges if it is situated between two electrodes (even if they are coated) supplied with high voltage [3]. In this type of partial discharge, are included corona effect, glow (plasma formed by the passage of electric current through a gas) and sliding discharges.

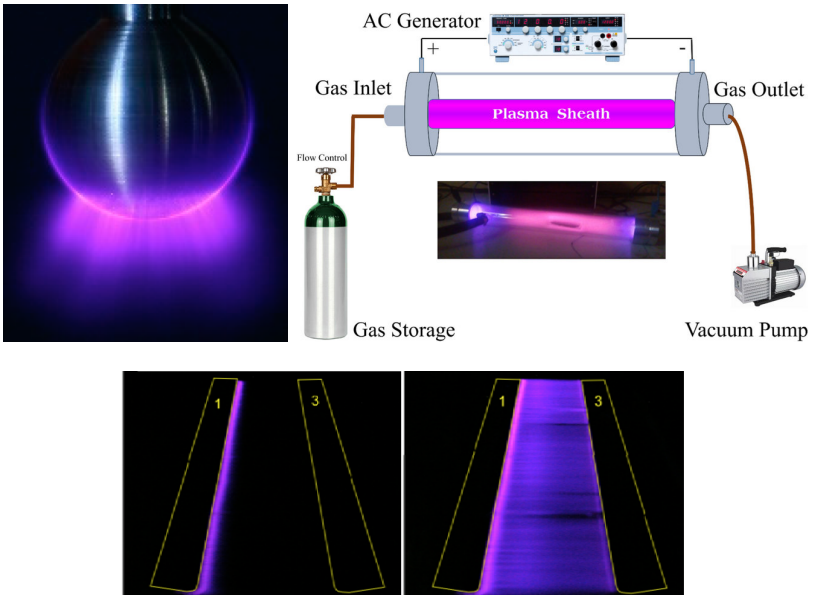

Figure 4: External partial discharges. Source: [6], [7], [8]

2.2.2 Corona effect and electric arc

From the types of partial discharges that are shown in subsection 2.2.1, this project shall be focused on the external partial discharges, specially, on corona effect and electric arc in aeronautical wires. Corona effect is a type of partial discharge that occurs when electric current flows through a gaseous medium (in this case air), due to ionization of the gas. However, the nature of discharges can vary depending on voltage and current is applied to the electrode [3]. To understand better which are the phases of the nature of partial discharges, it is represented the voltage-current curve.

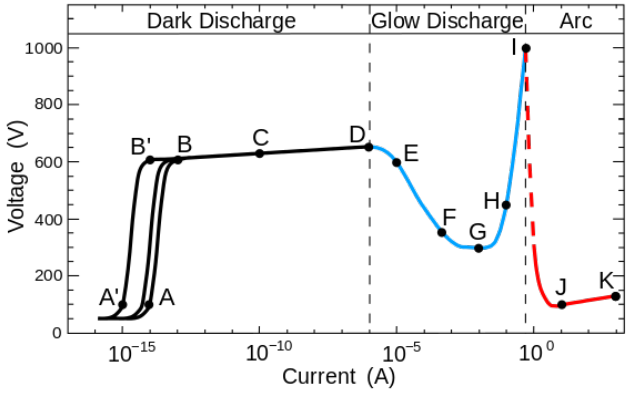

Figure 5: Nature of partial discharges. Source: [9]

In figure 5, it is possible to differentiate three phases. In phase I (A-D), also known as Townsend discharge, is a gas ionisation process where free electrons are accelerated by an electric field, collide with gas molecules, and consequently free additional electrons. The result is an avalanche multiplication that permits electrical conduction through the gas. The discharge requires a source of free electrons and a significant electric field; without both, the phenomenon does not occur. Here in this phase, corona effect appears.

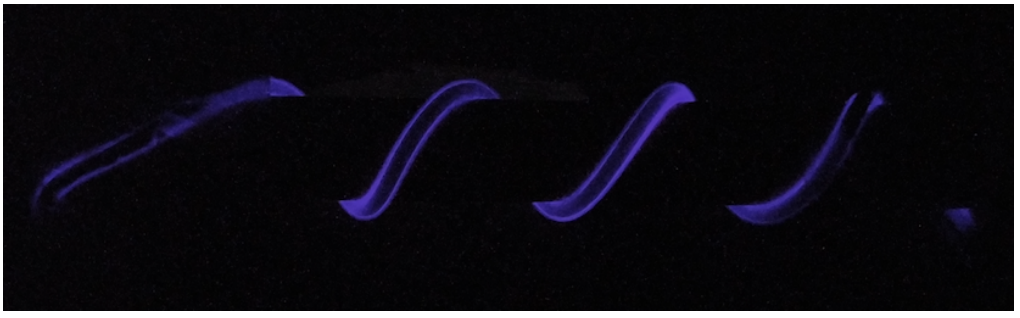

Figure 6: Corona effect in a twisted wire.

Phase II (D-I), also called glow discharge, occurs once the breakdown voltage is reached. The voltage across the electrodes suddenly drops and the current increases to milliampere range.

Finally, phase III (I-K) or arc discharge, a great amount of radiation is emitted and it is caused by the electrical breakdown of the gas that produces a prolonged electrical discharge and the current increases to amperes range.

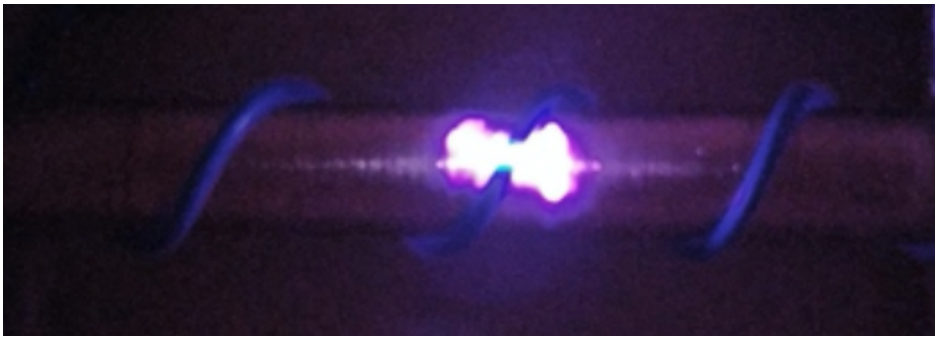

Figure 7: Electric arc in a damaged twisted wire.

In both figures, 6 and 7, the experiment was made twisting a wire in a cylindrical section copper bar and applying high voltage through the circuit. The copper bar was connected to ground in order to make appear the corona effect because, as explained, partial discharges come up when high voltage is applied between two electrodes with different potential.

2.2.3 Effect of pressure on partial discharges

It is important to highlight the relevance that has pressure on the behaviour of partial discharges when it is varied. As the study is related to aircrafts, pressure must to be taken into account. From ISO 2533:1975, it is known that when increasing altitude, consequently, pressure decreases.

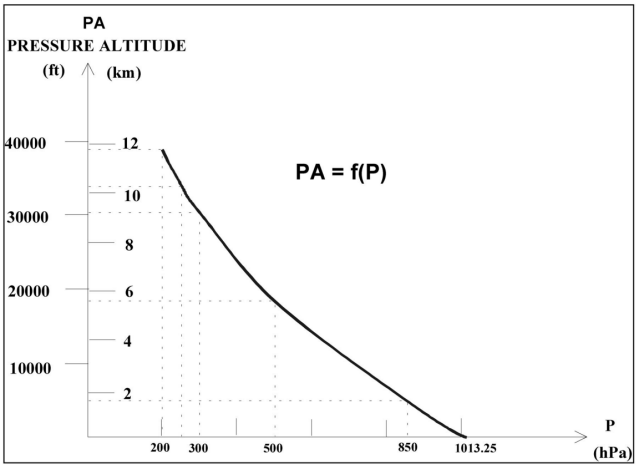

Figure 8: Pressure altitude versus pressure. Source: [10]

In 1889, Friedrich Paschen studied the breakdown voltage of parallel plates in a gas as a function of pressure and gap distance (Paschen Law). The voltage necessary to arc across the gap decreased up to a point as the pressure was reduced. It then increased, gradually exceeding its original value. He also found that decreasing the gap with normal pressure caused the same behavior in the voltage needed to cause an arc.

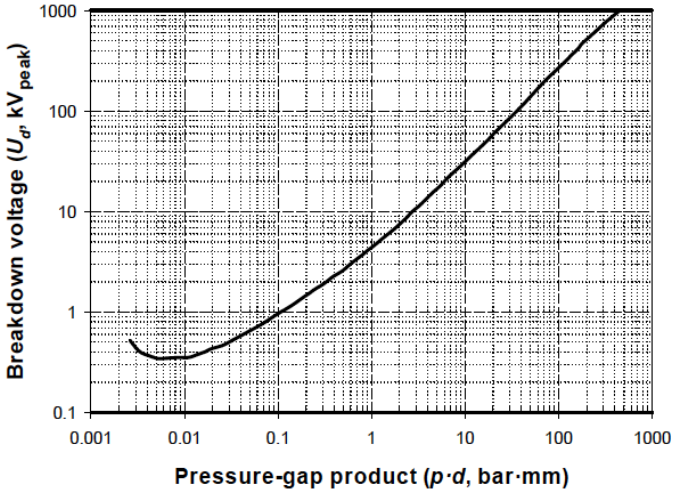

Figure 9: Paschen Curve. Source: [11]

In the curve from Figure 9, we can see clearly three points of interest. The left side corresponds to small pressure times distance, it means that that there are not enough molecules or atoms between the electrodes or exists a small distance between electrodes. Then, the probability for an electron to collide with molecules or atoms is very low and the voltage required to breakdown could tend to infinity. On the right side, shows a very

high value of pressure times distance, meaning that there are too many molecules between electrode. Nevertheless, the mean free path is reduced so that electrons do not gain enough velocity to ionize other atoms or molecules. Also, the required voltage to breakdown shall tend to infinite. Finally, the minimum value in the curve corresponds to the pressure times distance at which the breakdown voltage shall be the minimum [3].

However, Paschen's Law has some drawbacks when it is used for high voltage applications. It only applies for breakdown conditions, neglects space charge effects, and is only applicable to geometries with uniform electric fields. Most of the practical gaps are non-uniform and partial discharges might appear before a disruptive discharge is formed. Nevertheless, it can give an idea since it shows a tendency of the behaviour of gaseous insulation [11].

2.2.4 Consequences

As a consequence of partial discharges such as momentary short-circuit arcs, could thermally char the wire insulation or also known as pyrolysis (that is the thermal decomposition of material at elevated temperatures in an inert atmosphere). This charred material being conductive could propagate along the wire through continuous pyrolization of the insulation, commonly in polyimides, and if the arcing wire is part of a multiple wire bundle, the polyimide insulation of other wires within the bundle may become thermally charred and start to flash over. Therefore, arc tracking may lead to complete failure of an entire wire bundle or harness [17].

Partial discharges, can lead to system or component failure which is able to cause, in the worst case, ignition of the components involved in the affected system by the arc fault and spread the fire through the wires or the flammable materials to other parts of the aircraft. Usually, In-flight fires are originated in hidden areas of the aircraft, such as the attic above the cabin ceiling, beneath the floor, in or around the lavatories, or at similar locations that are not easily accessible by the crew [18]. For instance, in 1998, the Swissair Flight 111 which was a scheduled international passenger flight from John F. Kennedy International Airport in New York City, United States, to Cointrin International Airport in Geneva, Switzerland, had an accident due to loss of control and spatial disorientation caused by a short circuit and consequently fire ignition from the entertainment systems.

Also, there are several events that has been collected from a survey related to arc tracking on aerospace cables and wires [19], such as the TWA Lockheed L1O11 in August 1972, Bristol Helicopter A5332 L, Monarch Airlines Boeing 757 in January 1985 and again by B. A. Lockheed L1O11 in July 1989 that were the first incidents on cables due to arc tracking. The failures were analyzed by different aircraft organizations in Europe and in the USA. Some groups developed new test equipment to evaluate the recorded phenomenon, others simply banned the use of polyimide cable insulation considering other alternatives.

2.2.5 Prevention

Several measures are available to prevent or reduce partial discharge events, depending on their origin. In most cases, changing the design can help prevent the formation of locally higher electric fields, which are the primary cause of PD. The following measures have proved to be useful according to [2].

- Preventing decontamination of insulation material during **production** (conductive deposits, swarf, entrapped air or moisture).
- Rounding sharp tips and edges (field homogenization) to prevent the concentration of field lines.
- Optimizing the winding head shape (higher filling level without damaging the wires by pressure or wire tension).
- Increasing air gaps and creepage distances (e.g. in the event of sliding discharges) to reduce the field strength (voltage drop per distance).
- Through potting (free of voids or bubbles, e.g. under vacuum and by using inert gas, pipette filling from bottom to top, ascending potting compound).
- Increasing insulation layer thickness.
- Using materials that have a higher creepage current resistance (higher CTI value) or that are less prone to damage from partial discharge.
- Field control by using partially conductive coatings (e.g. semi-conductive surface insulating materials, paints acting as voltage controlled resistor VCR).

- Avoiding large ϵ_r (**relative permittivity of the medium**) when using two dielectrics. Materials with high dielectric constants break down more easily when subjected to intense electric fields, than do materials with low dielectric constants.
- Determining air gaps and creepage distances based on the application area (Paschen Law).

2.3 Regulations

Depending on the conditions which arc tracking is being generated, it is possible to differentiate two types. On one hand, dry arc tracking occurs in dry conditions when one or more conductors are shorted as a result of abrasion from the aircraft structure, wire to wire abrasion, installation error or battle damage. In wires using aromatic polyimide insulating material this can lead to carbon arc tracking. On the other hand, wet arc tracking occurs when contaminating moisture or aircraft fluids create a short circuit between an exposed conductor and the aircraft structure or an adjacent exposed conductor at a different potential. In wires using aromatic polyimide insulating material this can lead to carbon arc tracking [12].

The experimental part of this project has been inspired mainly in two standards which are focused on wet arc tracking, ASTM D2303 [13] and IEC-60587 [14], and show methodologies for evaluating resistance to tracking and erosion of insulating materials under severe ambient conditions using inclined plane samples. However, there are standards test methods that may be interesting to perform with other contaminants such as dust and fog (according to ASTM D2132 [15]) or conductive liquid drops (according to ASTM D3638 [16]) that are found in aircrafts during daily operation.

2.4 Methodologies

This section explains the different methodologies that have been carried out by different researchers or regulations when analyzing and detecting partial discharges during experiments. Also, as explained in the previous point, attempts have been made to follow the ASTM and IEC standards to carry out the tests and, in some of them, contaminants have been used to simulate a real case and verify that the sample being analyzed certainly passes the regulations. However, there are other methods that simulate a real case and

could advance the appearance of partial discharges, such as the case that the cable is broken among other methods that have been used by different research groups.

2.4.1 Proposals

Josef Hanson and Dieter Koenig in 1997 [23], proposed an electronic schema to perform tests of 'air tracking' on cables for space applications. They wanted to know more about the phenomena responsible for the fault arc behavior. In figure 10 it is shown the electronics and materials used for the experiments.

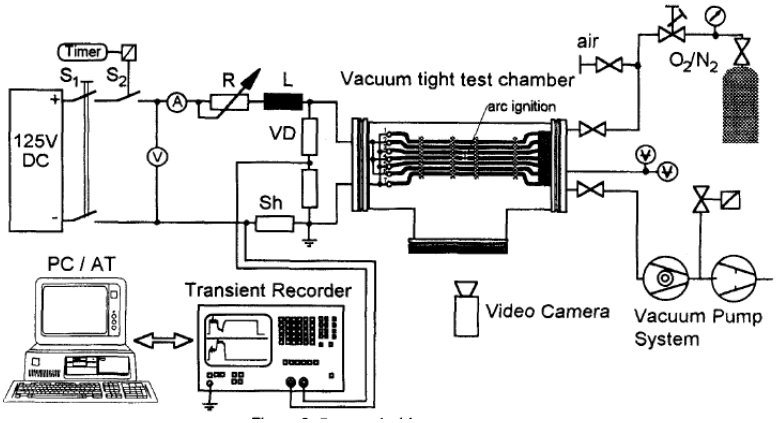

Figure 10: Experimental Set-Up proposed by Josef Hanson and Dieter Koenig. Source: [23]

The samples they used started with a well defined initiation of a fault arc with the help of a thin metallic filament (ignition wire) between two predamaged cables. The test tends to study the consequences of a burning fault arc and to find the fault arc resistance of the cable insulation. The test voltage is quasi-constant in the range of 125 to 132 V dc, while the test current is adopted to the rated current of each cable. The test specimen consists of an assembly of seven cables (200 to 250 mm long) cut from a continuous piece. Cables No. 3 and 4 are predamaged and short circuited with a metallic filament [23]. In figure 11 it is possible to see the disposition of the cables.

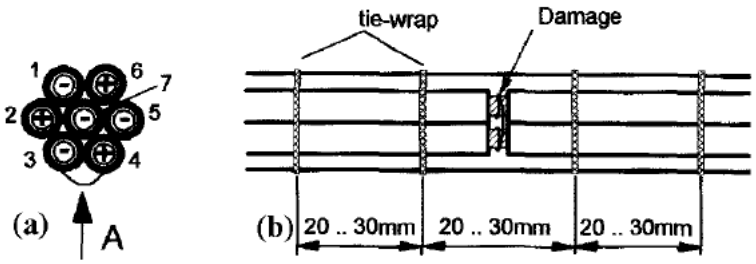

Figure 11: Cables disposition. a) Cross section view of the sample. b) View on arrow. Source: [23]

Benjamin Cella in his doctoral thesis [3], proposed the schema as seen in figure 12 to study partial discharges in different samples, among them the twisted pair of enameled wires. Even though Cella studied the three types of defects (internal, external and corona), it is interesting the methodology he followed to study the external defect which it is directly related to this project.

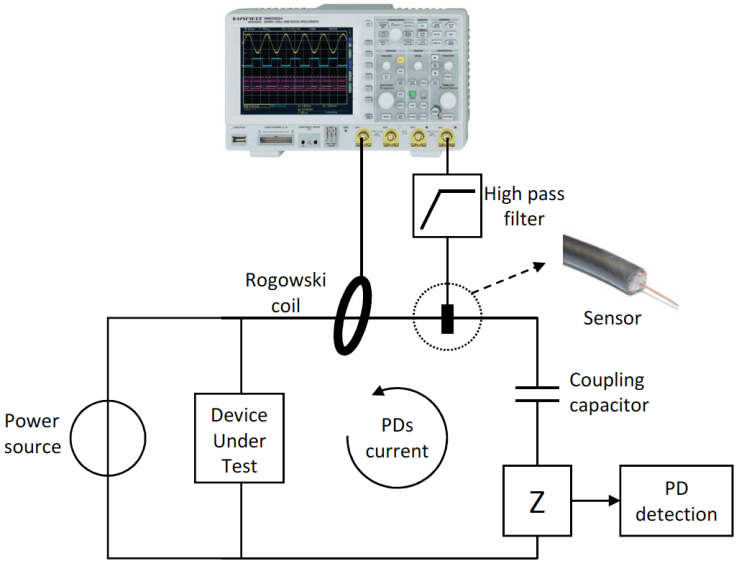

Figure 12: Measurement setup proposed by Benjamin Cella. Source: [3]

Experimental results are obtained by using radio-frequency detection due to the electromagnetic wave emission released from the samples because of the partial discharges. This method uses an antenna and an oscilloscope or spectrum analyzer. Also the results can be seen directly by optical detection due to the ionization of the air surrounding the wire. The sample used in this proposal it is shown in the following figure.

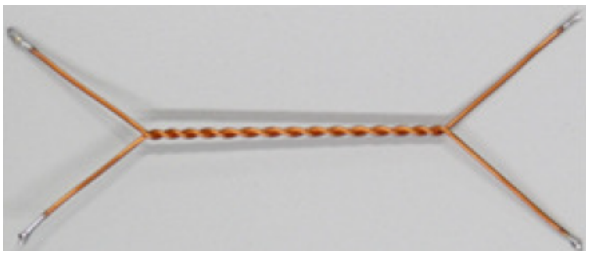

Figure 13: Twisted pair of enameled wires. Source: [3]

The materials are applied carefully on each sample to create the appropriate defects. Some of the insulating materials, such as enameled wire, were already applied. For these materials, the defects were created by modifying their geometry (e.g. twisting them together to create external defects). This material is tested, using the standard [24], by twisting two enameled wires around each other. [3]

H. El Bayda, F. Valensi, M. Masquère and A. Gleizes developed a circuit to create a fault arc between two cables for an adjustable period of time. The generator delivers continuous power with current regulation adjustable up to 100 A with a voltage of 110 V. This late value corresponds to the case of operating in open loop: once the arc is established the voltage drops to values depending mainly on the electrodes distance and nature. A commutation box using two Insulated Gate Bipolar Transistor (IGBT) transistors driven by a computer was operated via an interface system. It allows shifting the circuit from a first loop containing only the generator and a ballast resistance to the working circuit containing the cables during normal operation conditions [25].

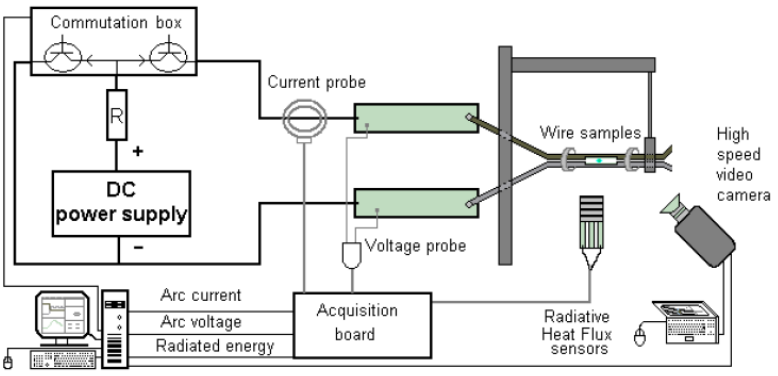

Figure 14: Experimental Set-Up proposed by El Bayda et al. Source: [25]

The procedure is first to wait for current stabilization and then to trig the shift to the working circuit. The control unit allows duration to be modified with steps of 10 ms, up to

9.9 s. As no high voltage is used for arc initiation, a specific procedure was developed for arc creation. For each experiment, the insulating sheath wrapping the cable was removed on one half of each wire, so that the two metallic cores can be placed in contact to each other. Two straps were used to bond the wires together at both end of the bare metal portion.

Two kinds of arc ignition were tested and used, corresponding to two classical configurations. The first one corresponds to a wet ignition: a salted water drop was spread on the two cables contact area before the wires are powered on. The second ignition was obtained in dry conditions by introducing a small metal wire between the two metallic cores [25].

V. Degardin, L. Kone, P. Laly, M. Lienard and F. Valensi , have focused on the study of the spectral components of the arc in the high frequency band, between 1 and 30 MHz. Also, they have proposed a Thevenin generator equivalent to the arc, allowing to determine the disturbing current and voltage spectral density at any point of the power network. This approach can be used to improve the efficiency of actual breakers and also to be able to predict interference between the disturbing signals due to this arc and sensitive control-command systems. [22]

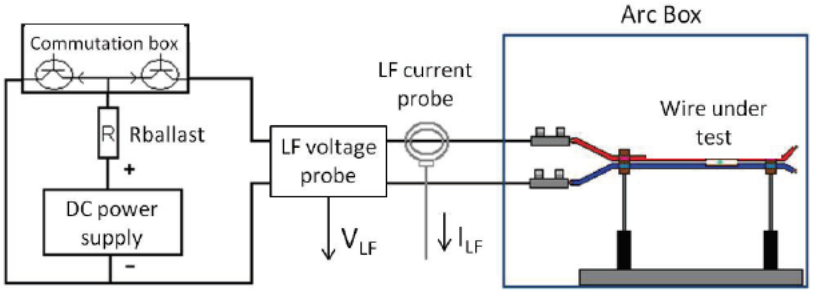

Figure 15: Experimental Set-Up proposed by T. André et al. for LF. Source: [22]

In figure 15, the arc is initiated between two wires whose part of the insulation has been first removed. To facilitate the arc ignition, a drop of salted water and a small and thin copper wire are placed in the contact zone of the two wires. The DC power supply delivers a voltage of 110 V, with current regulation up to 100 A.

A commutation box using two Insulated Gate Bipolar Transistor transistors driven by a computer was operated via an interface system. It allows shifting the circuit from a

first loop containing only the generator and a ballast resistance to the working circuit containing the cables during normal operation conditions. The procedure is first to wait for current stabilization and then to trig the switch to supply the working circuit.

In the zone where the arc will occur, the 2 conductors are placed in a box, named as "arc box". A DC/low frequency (LF) current probe and a high voltage differential probe having high input impedance are inserted in the feeding circuit to identify the LF current and voltage variation and thus the various phases of the arc. [22]

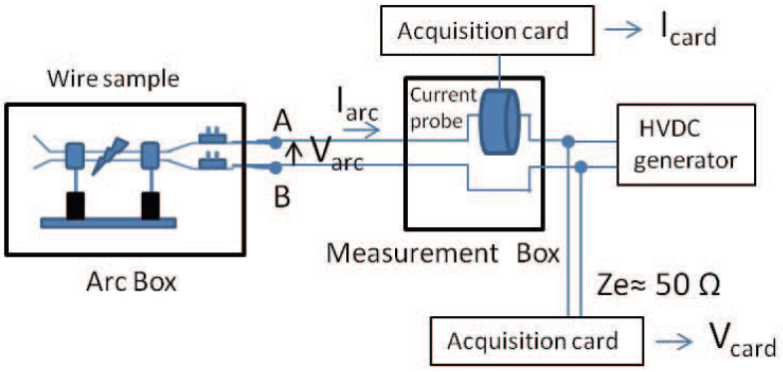

Figure 16: Experimental Set-Up proposed by T. André et al. for HF. Source: [22]

Regarding to the HF experimental set-up, the output of the arc box is now connected to a "measurement box" in which HF current and voltage will be measured. To measure the HF current, a probe which can withstand a DC current up to 350 A has been put around one wire of the power line, its transfer impedance being 1Ω in the 100 kHz- 30 MHz frequency band. Therefore, the distance between the 2 wires of the power line must be locally increased, leading to a change of the characteristic impedance of the line. Besides, correction factors have to be introduced to deduce, from the measured data Vcard and Icard, the voltage and current delivered by the arc tracking. A high band pass filter and clipping circuits protect the acquisition card, of 50Ω input impedance, against possible pulses of very high amplitude. This sampling card also presents an input impedance of 50 Ω and must thus be placed beyond the current probe, as shown in fig 16. All LF and HF acquisition cards are synchronized. [22]

T André, F Valensi, P Teulet, Y Cressault, T Zink and R Caussé [26] carried out different destructive tests of the samples in order to quantify the power transfers

from the tracking arc to the environment in AC circuit at atmospheric pressure. They proposed a circuit, as seen in figure 17, in which two aeronautical cables are connected to a phase of the AC circuit and the objective was to evaluate the various terms of power, based on experimental measurements such as current, voltage, radiated flux and mass loss.

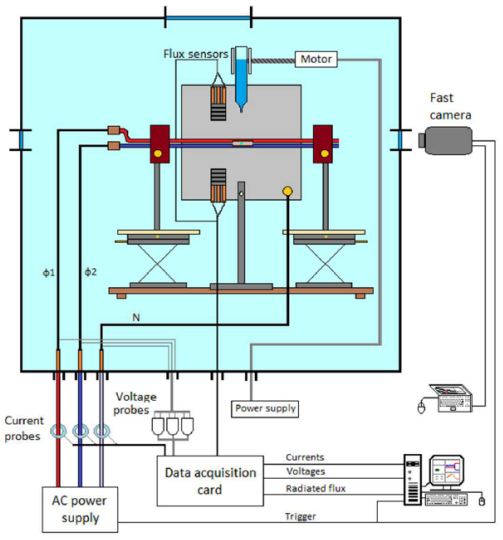

Figure 17: Experimental Set-Up proposed by T. André et al. Source: [26]

The procedure they followed was to strip the insulating sheath wrapping of the metal core on each cable and then the two cables are bond together so that the two stripped areas are close to contact.Each cable is connected to one phase. The ignition is facilitated with droplets of salted water (0.7% of NaCl) falling from a vial held above the stripped zone of the cables (this system works with a motor). The tests are carried out in a cylindrical chamber, at atmospheric pressure. Tests in AC with a 230 V open-circuit phase-to-neutral voltage have been done for the three cable types and for three current values: 175 A, 245 A, and 350 A. The frequency is 800 Hz. An aluminum plate (10cm × 10cm, 1.2 mm thick), representing the fuselage, is placed near the cables and connected to the neutral. [26]

Rui Rui and Ian Cotton, have investigated the influence of low pressure environment on the number of magnitude of partial discharges, the tests have been carried out in an environment chamber which simulates the low pressure environment in an aircraft. The samples that have been used consist of one pair of twisted insulated wires and a piece of insulated wire wound with a plain metallic conductor. In figure 18 it is possible to see the wire disposition. Sample 1 and 2 are the twisted pair insulated wires and sample 3 is the

insulated wire wound.

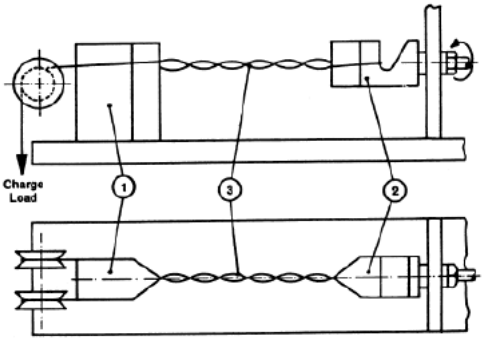

Figure 18: Sample proposed by Rui et al. Source: [27]

The standard laboratory method used for partial discharge detection is described in IEC 60270 [30] and ASTM D1868 [31]. A number of alternative configurations of detection circuit are available but all rely on a circuit of the type shown in Figure 3. An AC supply energizes the circuit, typically at 50 or 60Hz. A voltage divider is used to measure the voltage across the test object which is typically a capacitive load. Partial discharge pulses that are produced within the test object ideally flow round the loop formed by the test object and the blocking capacitance / LCR impedance. The output of the LCR impedance is a voltage pulse that has a magnitude that is proportional to the magnitude of the partial discharge. Through a calibration process, insulation systems can be shown to be free of partial discharge to a level of around 5pC. [27]

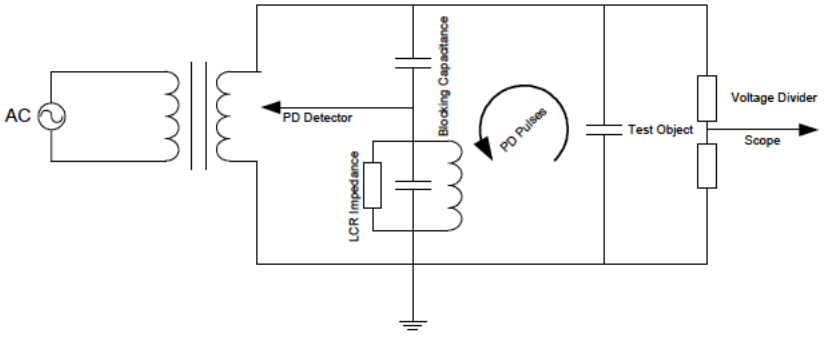

Figure 19: Experimental Set-Up proposed by Rui et al. Source: [27]

Athanasios C. Mermigkas, David Clark and A. Manu Haddad, use the approach that fits better with this project since both projects are studying the same phenomenon for high altitude in electric aircraft applications. However, the architecture is slightly different because of the modular data-acquisition system which enables to control and monitor temperature and pressure via optical link to the main control PC as shown in fig 20. Samples are twisted pair cables that has been extracted from a passenger aircraft.

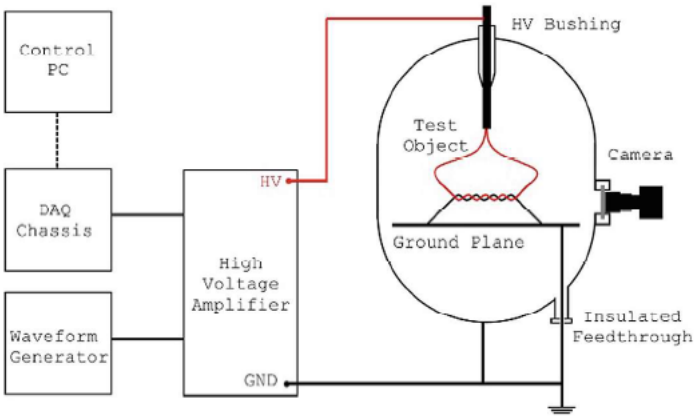

Figure 20: Experimental Set-Up proposed by Mermigkas et al. Source: [29]

In the following table, it is possible to analyze which are the advantages or the drawbacks between the proposals listed before, considering the material available and the less cost to execute the experiments.

Proposal	**Vacuum test**	**Initiation of a fault arc**	**Wire Materials**
Josef Hanson et al.	Yes	Pre-damaged cables and ignition wire	PI (polyimid), PTFE (polytetrafluoroethylene), PFA (perfluoroakoxy) and FEP (tetrafluoroethylene hexafluoropropylene).
Benjamin Cella	Yes	Twisted pair sample	Copper and polyurethane (PU)
El Bayda et al.	No	Wet ignition and ignition wire	Copper and PTFE
V. Degardin et al.	Yes	Pre-damaged cables	Copper
T. André et al.	No	Wet ignition and pre-damaged cables	Aluminium and copper, polyimide layer wrapped with a sheath of PTFE
Rui Rui et al.	Yes	Twisted pair sample	Polyimide wires and Kapton
Mermigkas et al.	Yes	Twisted pair sample	Nominal insulation rating of 600V (extracted from passenger aircraft)

Table 1: Features of each proposal.

2.4.2 Partial discharges detection

From previous subsection, one of important characteristics of partial discharges to highlight is that they emit electromagnetic radiation and this allows them to be easily detected using an antenna. Also, by ionizing the gas around the cable, the partial discharges emit ultraviolet (UV) light and they could be detected in a visual way. The following points

describe different methods for detecting partial discharges according to [3].

- **Standard electric detection**

  This method uses the charge displacement which is the measurement of the current flowing into a conductor.

- **Radio-Frequency detection**

  This method uses an antenna, and is mainly based on wave shape recognition and analysis. The easiest method is to connect an oscilloscope or a spectrum analyzer to the antenna and analyze the waves released by partial discharges .

- **Visual detection**

  This method allows to detect visually partial discharges from a camera or a sensor capable to detect the ultraviolet light. For instance, in Figure 6, has been used visual detection to observe partial discharges generated in the wire.

In this project is going to be used the three ways to detect partial discharges.

2.5 Environmental impact

Regarding the environmental impact that can generate partial discharges, when this phenomenon occurs the chemical reaction can produce ozone [11]. Ozone (O_3) gas exists naturally in the stratosphere, where it is formed when the sun's ultraviolet rays irradiate oxygen (O_2). Naturally occurring electrical discharges (lightning) also can transform oxygen into ozone. Also it is found naturally at ground level, in concentrations of 20 to 35 parts per billion (ppb). Human activity also can generate ozone due to a chemical reaction between nitrogen oxides and some volatile organic compounds. Ozone is the principal ingredient of urban "smog" and is a major element of the air quality index .

Apart from ozone, PDs also create nitric acid in air. Nitric acid is a highly corrosive, strongly oxidizing acid. Inhalation exposure to nitric acid is a common occupational hazard as it easily forms a vapour at room temperature. Symptoms of inhalation exposure to nitric acid include a burning sensation, dry nose and throat, cough, chest pain, shortness of breath, headache and difficulty breathing [28].

2.6 Wiring materials for aerospace applications

From the first years of creation of the aviation, PVC/Nylon, polyimide-based insulation (MIL-81381) and materials similar to this, for instance Kapton, had been used on wires until 1960 when new composites involving polyimide such as TKT (PTFE/Polyimide/PTFE composite) and other materials as ETFE (Ethylene tetrafluoroethylene), emerged. Polyimide materials are lightweight, flexible and present a good resistant to heat and chemicals. However, later on in 1972, issues related to this kind of insulation materials started to appear, so it was decided to ban the use of polyimide cable insulation and use composite TKT and ETFE [19]. Also PVC/Nylon is no longer in use nowadays.

Designation	**Insulation Material**	**In use** [21]
M5086/1	PVC/Nylon	No
M81381	Kapton®	A319, A320, A330, A340
M22759/34	Cross-Linked ETFE	Yes
M22759/80	TKT	Yes
M22759/11	Teflon®(PTFE)	BAe 146, B747
M22759/18	Tefzel®(ETFE)	Yes

Table 2: Aircraft wiring. Source: [19]

According to [21], which is an online article written by an Australian pilot that along of his career and through experience, has managed to identify issues related to arc tracking and has gathered information about insulation materials and the importance of raising awareness about this phenomenon, Kapton®is still in use in Airbus aircrafts such as A319, A320, A330 and A340 manufactured before 2005. Also PTFE is still in use in BAe 146 and B747 aircrafts.

As seen in the previous subsections, the impact that could generate arc tracking in aircrafts is large and could be very dangerous for the passengers and the crew to fly in an aircraft without taking into account this phenomenon. For this, cables and wires must to be reliable. One of the most important characteristics that electrical equipment and systems must have, is the resistance to fire ignition. Federal Aviation Administration (FAA) has performed different experiments related to fire ignition on wires, including the most

used materials for aircraft wiring such as PVC/Nylon, TKT and ETFE. Trying different configurations, it was found that TKT is the most resistant to fire when subjected to a severe ignition source among the samples. Also, it was found that PVC/Nylon is the most flammable material [18].

Figure 21: PVC/Nylon fire ignition study. Source: [18]

According to the best practices for aircraft's EWIS (Electrical Wiring Interconnect System) from the FAA [20], when selecting wires for aeronautical purposes in order to avoid unanticipated failures, the wiring features should be the following:

- Wires must ensure that the size is capable of having sufficient mechanical strength.
- Also, they should not exceed allowable voltage drop levels.
- Wires must be protected by circuit protection devices to minimize distress to the electrical system and minimize hazard to the airplane in the event of wiring faults or serious malfunction of the system or connected equipment.
- Meet circuit current-carrying requirements.
- It is not advisable to use wires with less than 19 strands. Consideration should be given to the use of high-strength alloy conductors in small gauge wires to increase mechanical strength. As a general practice, wires smaller than 20 AWG should be provided with additional clamps and be grouped with at least three other wires.

- Provide additional support at terminations, such as connector grommets, strain relief clamps, shrinkable sleeving, or telescoping bushings.
- Should not be used when subject to excessive vibration, repeated bending, or frequent disconnection from screw termination.

Exist other requirements concerning to tin- and silver-plated copper conductors when are exposed to continuous operation at high temperatures. These are:

- For silver-plated conductors, degradation in the form of interstrand bonding, silver migration, and oxidation of the copper strands will occur with continuous operation near rated temperature, resulting in loss of wire flexibility. Also, due to potential fire hazard, silver-plated conductors shall not be used in areas where they are subject to contamination by ethylene glycol solutions (used as a de-icing fluid for windshields).
- For tin-plated conductors, tin-copper intermetallics will form, resulting in an increase in conductor resistance.
- Both tin- and silver-plated copper conductors will exhibit degraded solderability after exposure to continuous elevated temperature.

3 Experimental features

3.1 Introduction

Once the most important aspects of partial discharges have been explained, such as why they are caused, what consequences they can cause and why it is a phenomenon that must be taken into account when designing and manufacturing electronic components or cables whose purpose is for aeronautical use, we move on to the most experimental part of the project, since, in this section, it shall be seen what material and equipment has been used to carry out the experiments.

Before listing the materials, it is important to emphasize that the study shall be based on three types of tests, that is, samples (which are basically cables with materials that are currently used in aircraft) shall be subjected to different types of current. Experiments shall be done in alternating current and direct current (in positive and negative polarity) and it shall be seen how the cable behaves in front of partial discharges. For this, an electrical circuit must be designed and prepared, such that, depending on the source that is available, it can rectify the signal and create direct current from the alternating current or vice versa.

Finally, in this section, it shall be detailed point by point, which steps have been followed and what criteria it has been taken into account to take the experiments and give them as valid.

3.2 Equipment and materials

This section lists all the materials involved in the final setup and what equipment is used to take the measurements. However, it is not explained how they have been assembled between them since it shall be explained in detail in the following points.

First of all we have the voltage generator, although it is really an apparatus used to perform dielectric tests on alternating current of components and circuits, it is capable of generating 10 kV in AC at a frequency of 50 and 60 Hz. It is true that for carrying out an experiment in real conditions simulating the electrical system of an aircraft, the frequency should be 400 Hz. Nevertheless, the material available in the laboratory did not

allow it to be done. The possibility of using a function generator was considered, since it allows the frequency to be varied while maintaining the same signal, but the voltage that is generated is around units or at most tens and the experiments are intended to be carried out at high voltage, therefore, it is required a transformer block from low to high voltage.

To simulate the altitude at which the airplane flies, a vacuum chamber has been used which, by means of a pressure pump, it shall remove the air until reaching the desired pressure to perform the tests. The maximum pressure at which the tests shall be carried out is the atmospheric pressure at sea level (101325 Pa) and the minimum is 10 kPa that is equivalent to a 16 km of height from the Earth's surface. In general, commercial aircrafts fly at a height between 10 and 12 km, that would be equivalent to a pressure between 20 and 25 kPa, but there are certain private jets whose service ceiling is almost 16 km, so the study shall be between that pressure range. The vacuum chamber has an EVA rubber layer that ensures the hermetic seal and allows the pressure to be constant without losses between the lid and the container.

The electrical components required to form the circuit that converts alternating current into direct current are: diodes and capacitors. The diode acts as a half-wave rectifier, since depending on the threshold voltage and the direction in which it is placed, the voltage shall be positive or negative. On the other hand, the capacitor, which is an electrical component that stores electrical charge in the form of a potential difference, the space left by the diode corresponding to the negative part of the wave (or positive if negative voltage is allowed to pass) it will maintain the same voltage since the capacitor releases the electrical charge that has been previously stored. The chosen capacitor value ensures that the discharge time is as fast as it seems a continuous signal.

Finally, if it is recalled from subsection 2.4.2, there are three ways to detect partial discharges, these are by visual, electrical detection and by radio-frequency emissions that are generated by the discharges themselves. In this project, all three ways have been used to detect them, so the instruments that have been used are the oscilloscope and a camera. The advantage of the oscilloscope is that it has different channels and allows comparing two signals at the same time or more, depending on the channels that are selected, and

this has made it possible to compare the signal that comes from the antenna to detect radio frequency waves and the electrical signal from the circuit itself.

Figure 22: Electrical and RF detection of partial discharges.

For the visual detection of partial discharges using the camera, a 48-megapixel Xiaomi Redmi mobile phone has been used, allowing to obtain high-quality images of the ultraviolet light emitted by the ionization of the air surrounding the cable. In addition, the images have been taken with a high exposure time to absorb the largest number of photons and see the corona effect clearly.

3.3 Electrical circuit

As mentioned in the introduction, the experiments that are going to be carried out in this project, shall be based on different tests, that is, the sample shall be subjected to direct current with positive and negative polarity, and also it shall be subjected to alternating current. Regarding the high voltage generator that has been chosen, by default, it already provides alternating current, therefore, a rectifier block connected to the sample is not needed. The arrangement of the circuit to perform the tests in alternating current is shown in the following figure.

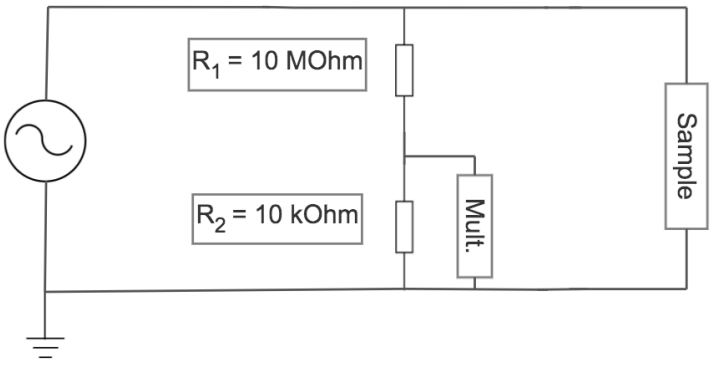

Figure 23: AC configuration.

It is possible to see that it has been used two resistors in series, one resistor of $R_1 = 10M\Omega$ and one resistor of $R_1 = 10k\Omega$. It is done due to the fact that the multimeter is not capable of reading kV, so with this setup and the multimeter connected in parallel to resistor R_2, it shall be able to read almost the same voltage as the source but divided by 1000. It means that, if the generator gives 1000 V, the multimeter shall read approximately 1 V. This enables to vary the voltage accurately to the desired amount.

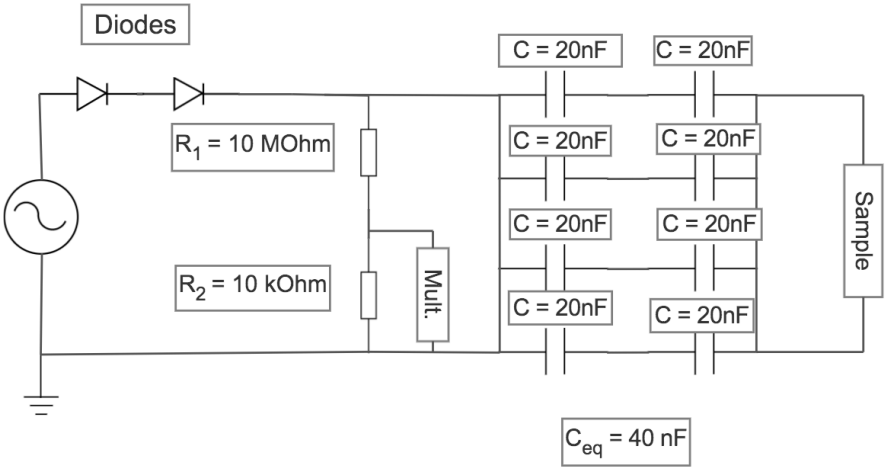

Figure 24: Positive DC configuration.

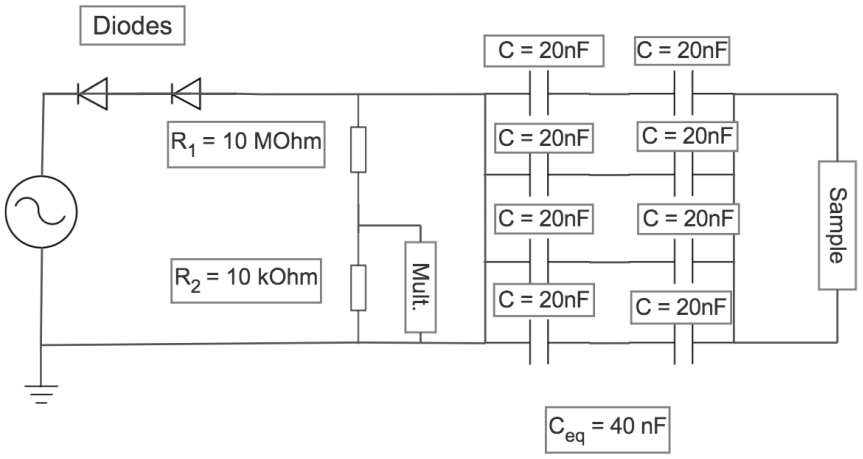

Figure 25: Negative DC configuration.

However, if the experiments are in direct current, to convert the signal, a total of eight 20 nF capacitors have been used, connected in parallel with two capacitors in series for each branch, to obtain an equivalent of 40nF. This allows us to rectify the signal and have direct current. To change the polarity of the signal, two diodes have been used in series whose maximum voltage that each can withstand is 20 kV, so depending of the polarity is desired, the diodes shall be positioned as shown in figures 24 and 25. It is known that if the experiments do not exceed 20 kV, it could be done with just one diode. Nevertheless, it has been used one more to not overload the diodes.

3.4 Experimental set-up

3.4.1 General set-up

The general setup is mainly composed by the signal converter circuit, including the high voltage source and the vacuum chamber with its respective pressure pump. A metal rod has been pierced through the middle of the lid thus allowing electricity to flow into the vacuum chamber, since tests will be carried out inside it. The connections are made using special cables for high voltage with crocodile clips at the ends to ensure that the connections are made correctly and do not form a short circuit (Figure 26). Two multimeters have been used to measure the voltage leaving the generator and the current in the circuit in order to collect the data and precisely control the voltage manually to detect the inception voltage that is when the corona effect begins to be visible.

Figure 26: Source and vacuum chamber.

On the other hand, it is essential to create a setup capable of placing the sample so that each time an experiment is to be carried out, it is in the same position and in the same conditions to obtain reliable data. Therefore, a wooden structure has been created that contains the sample inside, also it has made a compartment to put the mobile and to be able to obtain the images during the test (Figure 27). It is important that the structure allows the necessary connections to be made since the cable to be tested must be connected to high voltage and that the copper tube (in the case of the corona effect study) or the other extreme of the electrode (in the case of the electric arc study) they are connected to ground, which in this case shall be connected to the wall of the vacuum chamber being that it acts as a Faraday cage.

To prevent the vacuum chamber from being electrically charged with high voltage and for the safety of the person who is in charge of the tests, the chamber rests on a metal plate that acts as ground, so every time it is touched the chamber to make pressure changes or if it is wanted to be removed the structure from the inside, there will be no danger of high voltage discharge. Also, to increase security, the vacuum chamber has been placed inside a Faraday cage, in Figure 26 you can see how the setup finally looks.

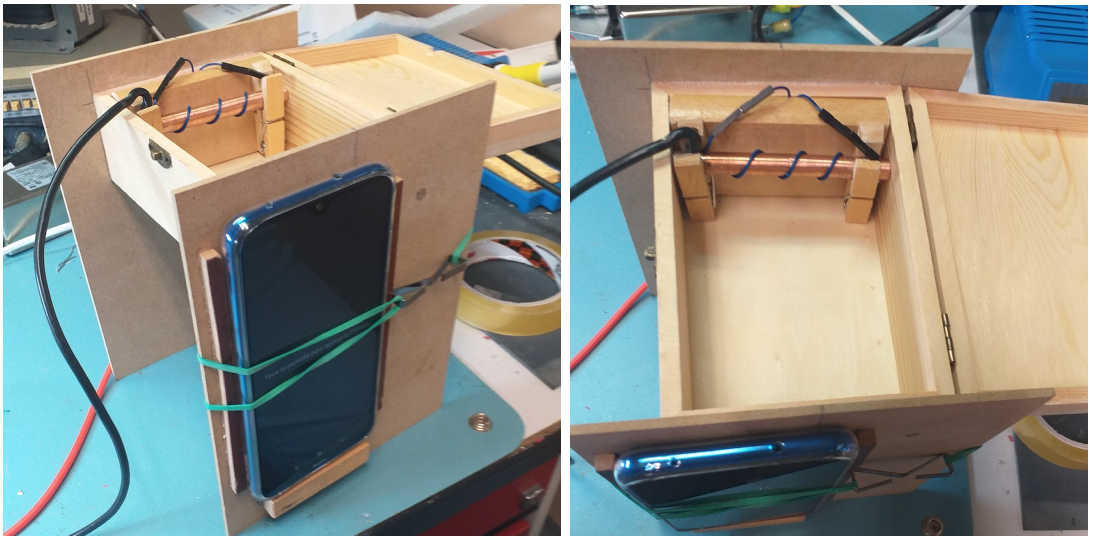

Figure 27: Structure for visual detection.

To carry out the measurements by radiofrequency, a circular antenna has been made that is positioned on the cover of the vacuum chamber, which is made of methacrylate and on that side it is the only place that shall receive the waves with higher intensity. The cable is passed through the Faraday cage until the antenna is connected to the oscilloscope on a specific channel. In another channel shall be the cable that connects the oscilloscope with the circuit in order to directly receive the signal and then be compared with that coming from the antenna.

Figure 28: Top of the lid: antenna and metal rod.

3.4.2 Corona detection set-up

As has been seen in the proposals section, the researchers, based on the regulations IEC 60270, ASTM D1868, IEC 60587 and ASTM D2303, have wanted to innovate new methods to detect partial discharges, either by adding fluids that allow the appearance of partial discharges to advance, or removing part of the insulating coat of the cables enabling the electrode to be directly exposed to the air. Table 1 lists the methods used.

In this project it is wanted to use different methods to see how the results vary in each case and to be able to get conclusions from it. The first sample, also called spike-plane method, will be a cable cut in half exposing the part that conducts electricity and placed at a certain distance from a plane that will be connected to ground (this distance shall be around 10 mm). The second sample will be the M22759/34 cable coiled in a copper tube without any defect and without any additive for the appearance of partial discharges. Finally, the third sample will have a defect in the insulating coat of the cable without any additive. The following figure shows how the samples are for detecting the corona effect on wires. Samples 2 and 3 shall have the same setup as it is shown in the image on the left while the image on the right it is the setup for sample 1.

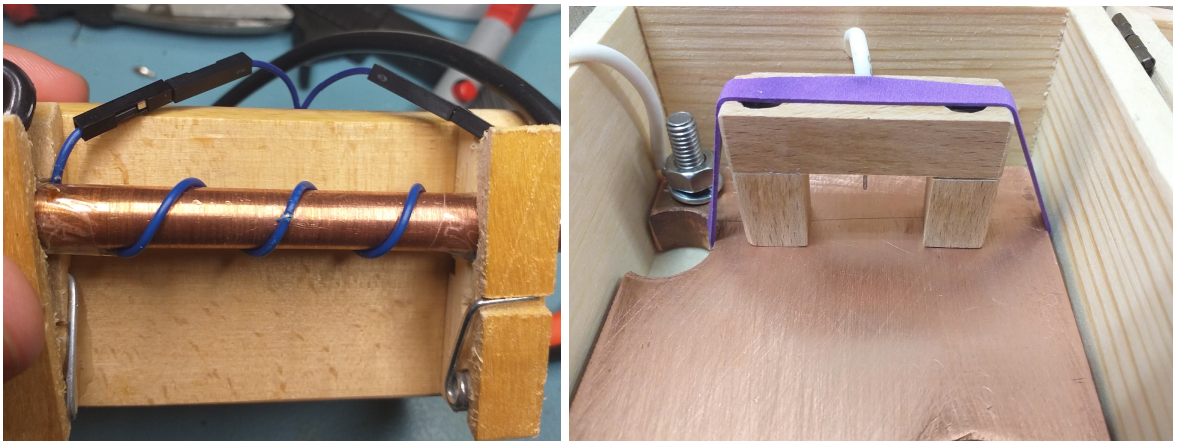

Figure 29: Corona detection setups.

3.4.3 Electric arc detection set-up

Although this experiment could be done with the same M22759 / 34 cable, it is wanted to do a different setup using two electrodes separated at a certain distance as can be seen in Figure 30. At one extreme of the electrodes the high voltage shall be connected and the other extreme shall be connected to ground. The idea is to obtain the breakdown voltage depending on the pressure and the distance at which the electrodes are separated as Paschen's law dictates.

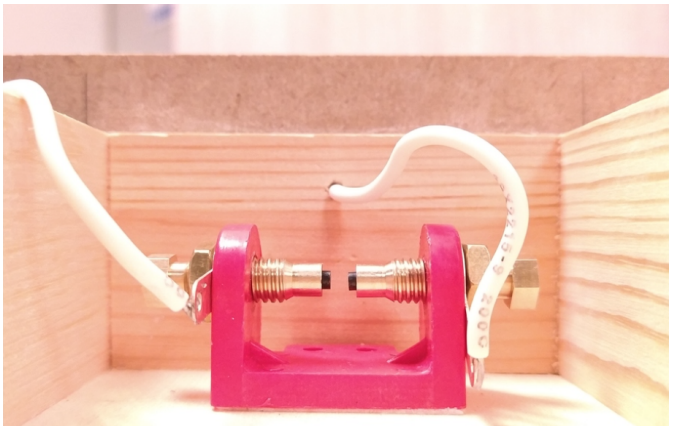

Figure 30: Arc detection setup.

3.5 Experimental procedure

As this project is based on research to prevent companies of the aerospace sector and companies that manufacture electrical components for aerospace purposes, it is wanted to raise awareness that this is a problem that could have serious consequences, therefore, it shall be obtained data mainly of the voltage at which the partial discharges appear, also called the inception voltage and the disappearing voltage, also called the extinction voltage, since partial discharges are detected at a certain voltage they could disappear even at a lower voltage than the one initially perceived. The current corresponding to each voltage obtained shall also be noted. The diagram shows the procedure to be followed.

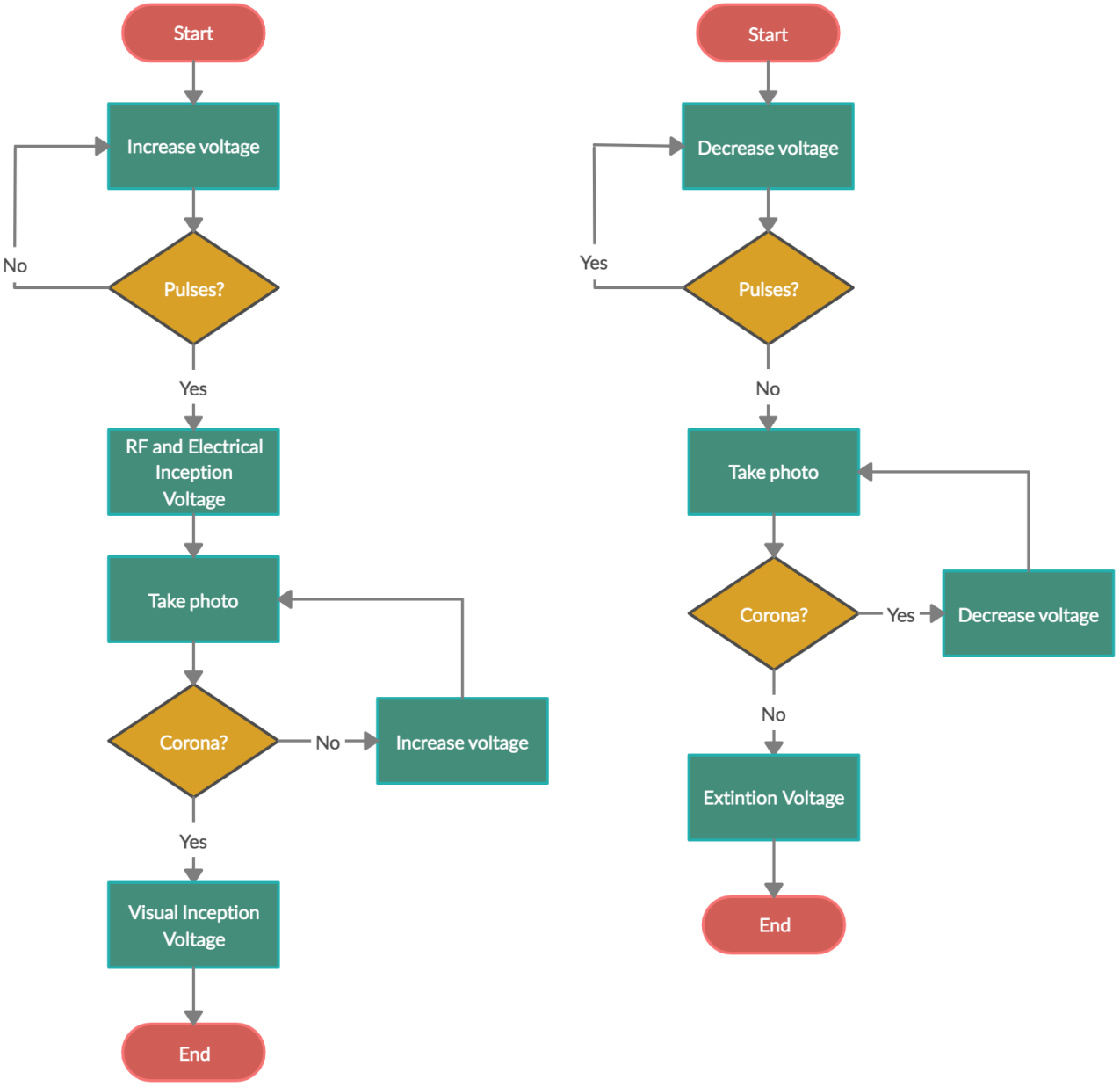

Figure 31: Experimental procedure flowchart.

- The first step is to increase the voltage from the source until pulses are detected. Both signals that come from the antenna (induced voltage) and the signal corresponding to the voltage drop in the resistance from the circuit, must present this phenomenon. The pulses generated by the partial discharges can be easily identified as these create an increase in voltage and can be seen as if they were peaks on the oscilloscope screen.

- Once the pulses have been detected from the oscilloscope, the voltage and intensity corresponding to that moment are collected. Besides, a photo is taken from the mobile that has been remotely controlled from the computer using software programmed in Linux. It is possible that the image shall not capture the corona effect since it has been seen that signal detection perceives the discharges earlier than the visual detection. Therefore, the voltage is increased until the effect is visually detected and the same data (voltage and current) is noted at that moment.

- The two previous points are the process that must be followed to identify the inception voltage, now the reverse process must be done to find the extinction voltage at which the partial discharges disappear since they can be more restrictive. Therefore, the voltage is lowered until the pulses can no longer be observed on the oscilloscope and the voltage and current are noted. To corroborate that there is no corona effect, a photo is taken again at that moment. In general, this last point is unnecessary since signal detection is more reliable than visually.

On the other hand, if it is wanted to detect the electric arc, the steps to follow are similar to the previous structure. However, it has been a little more complicated when taking the data since the source has an automatic shutdown mechanism when it detects arcing so it must to be very aware of the values of the voltage and current in the arcing instant. The procedure is based on raising the voltage until the pulses of the partial discharges appear, it is a phenomenon that happens before the arc appears, then the long exposure photo is taken (32 seconds) and voltage is risen slowly until the arc jumps and the voltage and current is taken at that moment.

4 Experimental results

4.1 Introduction

In this section, the experimental results are shown according to the methodology indicated in the previous point. In general, five tests have been carried out, three for the study of the corona effect, which, as it is known, the corona effect is a phenomenon that appears in the Townsend phase where the air is ionized due to the electron acceleration causing collisions between more molecules enabling an electrical conduction through the gas. Finally, two tests related to the last phase of the partial discharges, the electric arc, have been done.

4.2 Sample 1: Spike-Plane method

4.2.1 S1: Alternating current

In this experiment it was discovered that the partial discharges could be previously identified by using signal detection (antenna or voltage drop in a resistance at the end of the circuit) with the oscilloscope. Although it is one of the last tests carried out for the study, it was identified that the trend of extinction voltage when the sample is subjected to alternating current, follows an almost linear growth with respect to pressure. Furthermore, as can be seen in figure 32, the curve corresponding to the detection by antenna follows the same linear form. It was verified that in each pressure, the result for both methods does not exceed 5% relative error. In table 3, it is listed the values of the points that corresponds to each curve in figure 32.

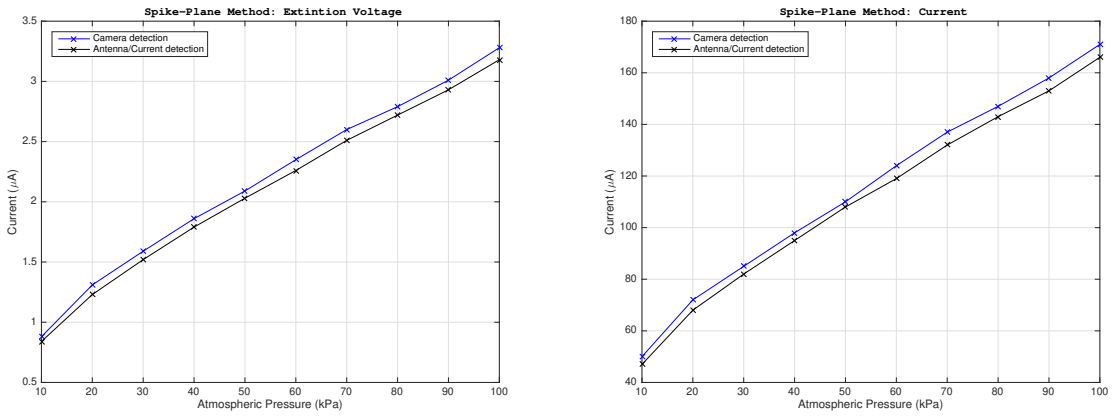

Figure 32: Spike-Plane test under alternating current.

	Visual Detection		Antenna Detection	
Pressure (kPa)	**CEV (kV-AC)**	**Current (μA)**	**CEV (kV-AC)**	**Current (μA)**
10	0.88	50	0.84	47
20	1.31	72	1.23	68
30	1.59	85	1.52	82
40	1.86	98	1.79	95
50	2.09	110	2.03	108
60	2.35	124	2.26	119
70	2.60	137	2.51	132
80	2.79	147	2.72	143
90	3.01	158	2.93	153
100	3.28	171	3.18	166

Table 3: Sample 1: AC results for visual and antenna detection.

The values obtained in this case are in root mean square value, so if it is wanted to be compared with a continuous signal, it would have to be multiplied each one by the root of two. In figure 33, the corona effect image was obtained at a pressure of 20 kPa, it can be seen that there is greater luminosity near the electrode because there is more electric charge creating more collisions between the molecules and therefore releasing the electrons. As exists a distance between electrodes, the charge carriers (they can be electrons or ions) cannot cross the space, therefore, when there are different charges and since the alternating current is composed of a positive half cycle and another negative, it causes a part of these charges to be directed towards the electrode and the other part to remain in a region of space creating collisions between particles due to the phenomenon of repulsion and diffusion. Also, a light beam can be observed that falls on the copper platform because certain electrons do manage to reach the other electrode that is at different potential.

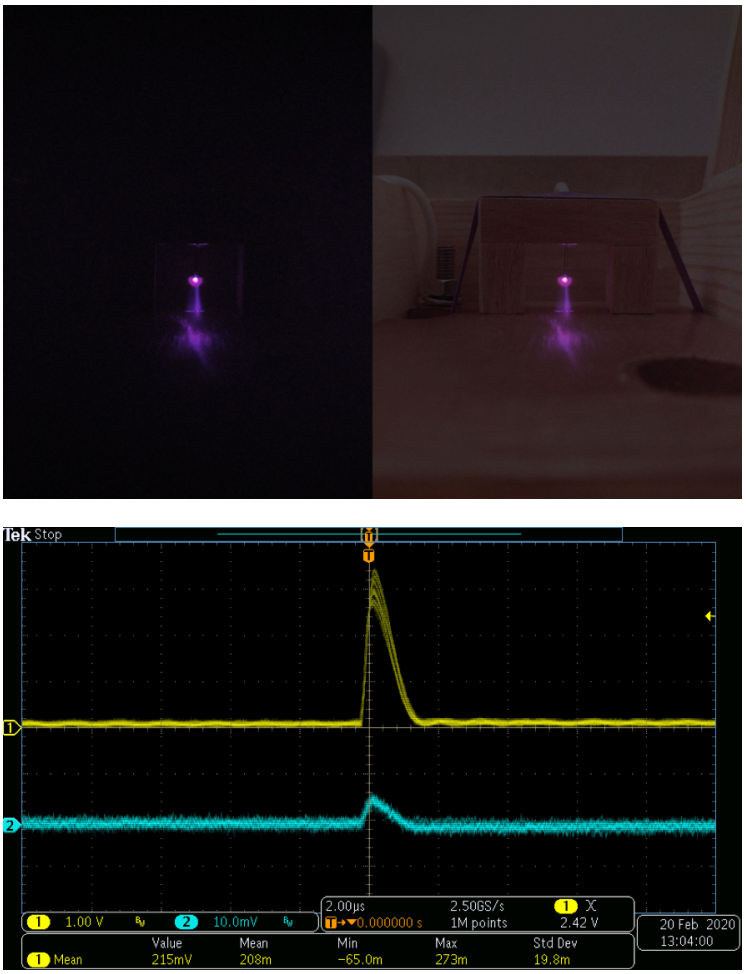

Figure 33: Visual and radio-frequency/electrical detection of spike-plane test.

Regarding the signal obtained and analyzed from the oscilloscope, it can be seen that the scale necessary to detect the signal coming from the antenna (blue signal) is 10 mV, while if the signal coming directly from the circuit is analyzed (signal yellow) is easily seen on a 1V scale. However, although the detection scale varies, partial discharges are detected at the same time by both signals, but one with greater intensity than the other. It is important to emphasize from the signals that these have been detected in the positive part of the wave, while the literature says that partial discharges are more likely to be shown in the negative part [6].

4.2.2 S1: Positive direct current

Once entering the DC tests, we will see that the behavior of the partial discharges are different compared to alternating current. Below, it is possible to see the extinction voltage and current graphs obtained during the tests for different pressures with their corresponding values listed in table 4.

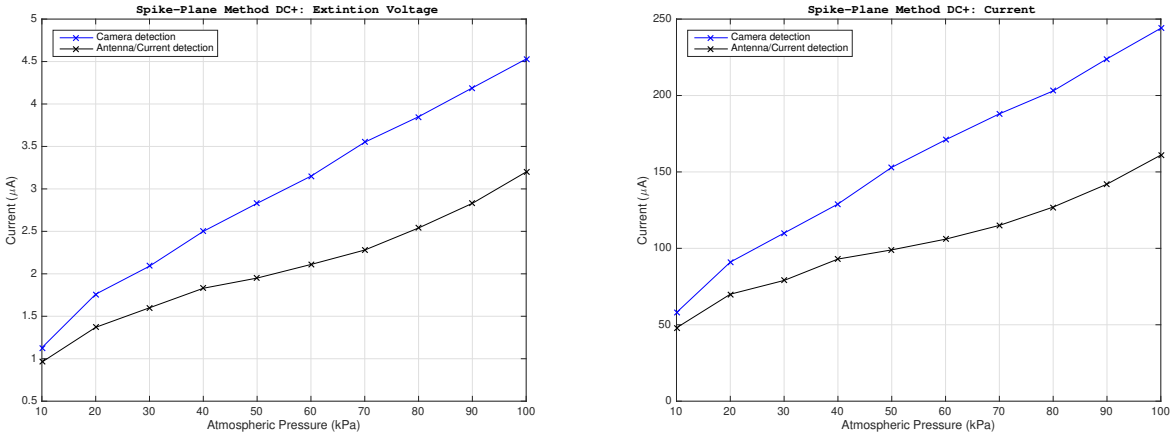

Figure 34: Spike-Plane test under positive direct current.

	Visual Detection		Antenna Detection	
Pressure (kPa)	**CEV (kV)**	**Current (μA)**	**CEV (kV)**	**Current (μA)**
10	1.13	58	0.96	48
20	1.76	91	1.37	70
30	2.09	110	1.60	79
40	2.50	129	1.83	93
50	2.83	153	1.95	99
60	3.15	171	2.11	106
70	3.55	188	2.28	115
80	3.85	203	2.54	127
90	4.19	224	2.83	142
100	4.53	244	3.20	161

Table 4: Sample 1: DC+ results for visual and antenna detection.

First, it should be said that the voltages at which partial discharges are detected are higher compared to those obtained in alternating current. Also, it is important to emphasize that as the pressure increases the lines corresponding to the values detected by both methods are separating, this means that the partial discharges are present long before they can be seen. At atmospheric pressure above sea level, the results from both methods differ 1.33 kV. Finally, in figure 35 that corresponds to visual detection, we see that the corona effect is visible throughout the electrode since the method we are considering does not contain the cable insulation and this makes the visibility greater and that can be detected even at lower voltages.

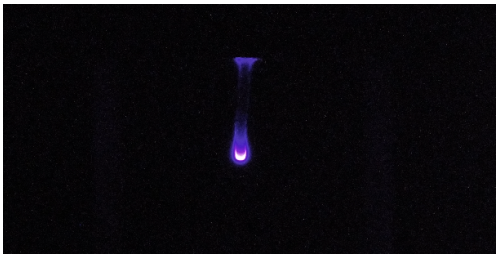

Figure 35: Spike-plane visual detection: DC+.

4.2.3 S1: Negative direct current

The results belonging to negative direct current using the spike-plane method are represented in figure 36 with their corresponding values that are listed in table 5.

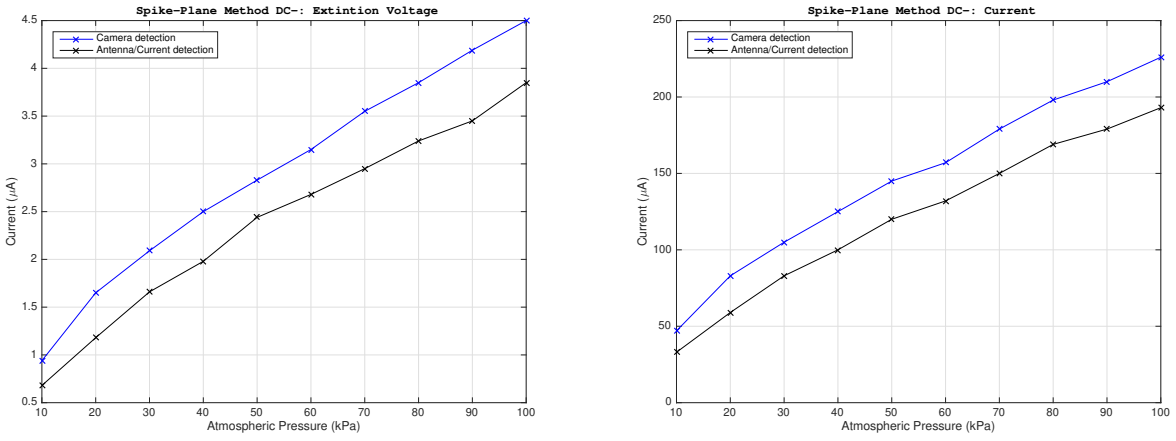

Figure 36: Spike-Plane test under negative direct current.

	Visual Detection		Antenna Detection	
Pressure (kPa)	**CEV (kV)**	**Current (μA)**	**CEV (kV)**	**Current (μA)**
10	0.94	47	0.68	33
20	1.65	83	1.18	59
30	2.09	105	1.66	83
40	2.50	125	1.98	100
50	2.83	145	2.44	120
60	3.15	157	2.68	132
70	3.55	179	2.95	159
80	3.85	198	3.24	169
90	4.19	210	3.45	179
100	4.50	226	3.85	193

Table 5: Sample 1: DC- results for visual and antenna detection.

In this case we see that a linear trend continues on the part of the two lines and that the method by antenna detection or by measuring the voltage drop in a series resistance to the circuit, continues to be detected previously than visually. The results obtained by the visual method are not so different from the case of positive direct current, however for the other case we see that the partial discharges are seen later than those detected in the positive DC. In figure 37, it is seen that unlike positive DC, the light is dimmer and that there is a clear difference due to polarization.

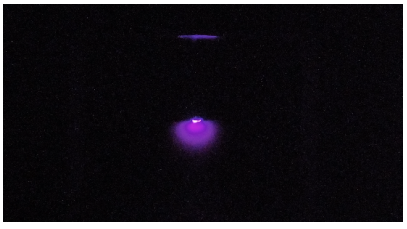

Figure 37: Spike-plane visual detection: DC-.

4.3 Sample 2: Cable coiled around a copper tube

In this test, the aeronautical cable M22759/34 has been used to subject it to alternating and direct current until partial discharges are detected, then, identify at which voltage these disappear. Extinction voltage can have a lower tension than the inception voltage,

so it is more restrictive and prudent to consider the one that is less. A high voltage will be applied exceeding the limits set by the manufacturer until corona effect is seen through camera.

4.3.1 S2: Aternating current

The results belonging to alternating current are represented in figure 38 with their corresponding values that are listed in table 6.

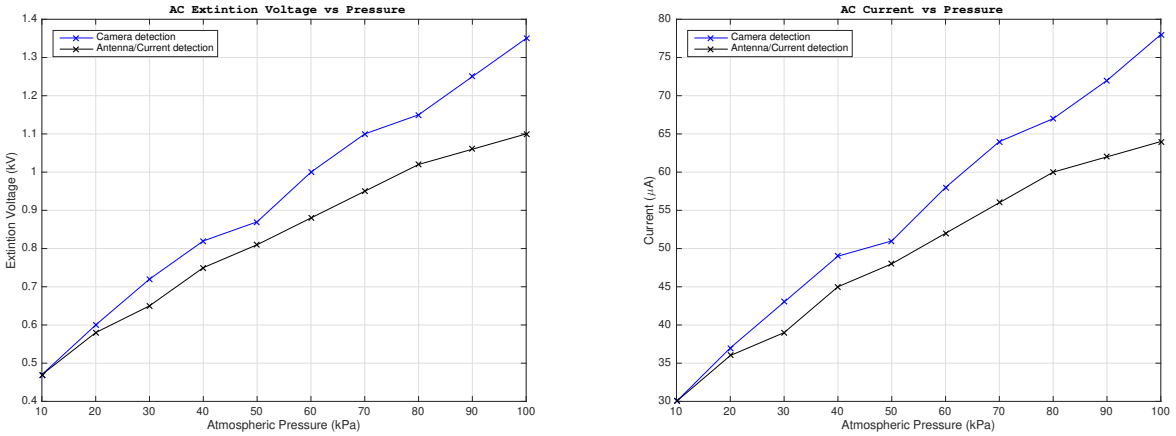

Figure 38: M22759/34 sample test without defect under alternating current.

	Visual Detection		Antenna Detection	
Pressure (kPa)	**CEV (kV-AC)**	**Current (μA)**	**CEV (kV-AC)**	**Current (μA)**
10	0.47	30	0.47	30
20	0.60	37	0.58	36
30	0.72	43	0.65	39
40	0.82	49	0.71	45
50	0.87	51	0.81	48
60	1.00	58	0.88	52
70	1.10	64	0.95	56
80	1.15	67	1.02	60
90	1.25	72	1.06	62
100	1.35	78	1.10	64

Table 6: Sample 2: AC results for visual and antenna detection.

It is interesting to see from the graphs, that the current trend also follows a linear behavior and the order of magnitude is micro amps. When taking the results, it was seen that if partial discharges appeared, the current and the applied voltage began to oscillate with more intensity, so the values collected in the tables are an average of different measures. Regarding visual detection, the luminosity of the corona effect on the cable under alternating current is quite striking. As for signal detection, it is first detected in the negative half wave by the circuit (yellow signal), while the antenna captures radio frequency waves with a fairly high frequency (purple signal). The scale used for the signal of the voltage drop has been 200 mV and for the signal coming from the antenna a scale of 10 mV.

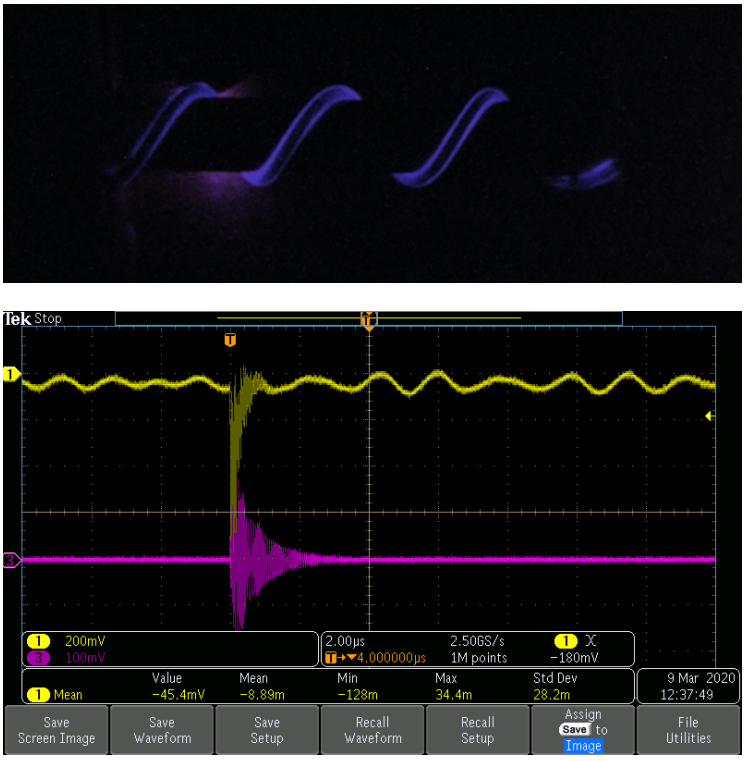

Figure 39: Visual and radio-frequency/electrical detection under AC current.

4.3.2 S2: Positive direct current

The results belonging to positive direct current for the aeronautical wire are represented in figure 40 with their corresponding values that are listed in table 7.

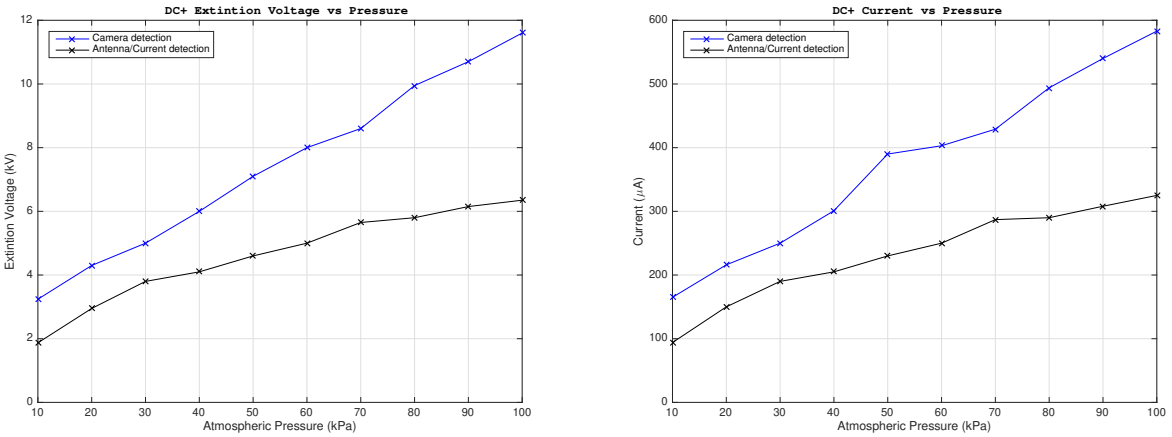

Figure 40: M22759/34 sample test without defect under positive direct current.

	Visual Detection		Antenna Detection	
Pressure (kPa)	**CEV (kV)**	**Current (μA)**	**CEV (kV)**	**Current (μA)**
10	3.24	165	1.87	94
20	4.30	216	2.95	150
30	5.00	250	3.80	190
40	6.00	301	4.10	205
50	7.10	390	4.60	230
60	8.00	403	5.00	250
70	8.60	429	5.65	287
80	9.95	494	5.80	290
90	10.70	540	6.15	308
100	11.60	583	6.35	325

Table 7: Sample 2: DC+ results for visual and antenna detection.

In the aeronautical wire, due to the effect that the insulating material causes on the conductor, the values obtained in both methods are slightly higher than sample 1 where we had the conductor discovered. As for example, if we see the section corresponding to 100 kPa, the voltage at which the partial discharges appear is 6.35 kV detected by the antenna and become visible at 11.60 kV. The values obtained for the visible method the corona effect was not as bright as in the case of alternating current, in figure 41 we see how it is quite complicated to see the corona effect, also that every time the inception

voltage was obtained the electric arc jumped. Analyzing the graphs, as in sample 1, the lines also tend to separate as the pressure increases.

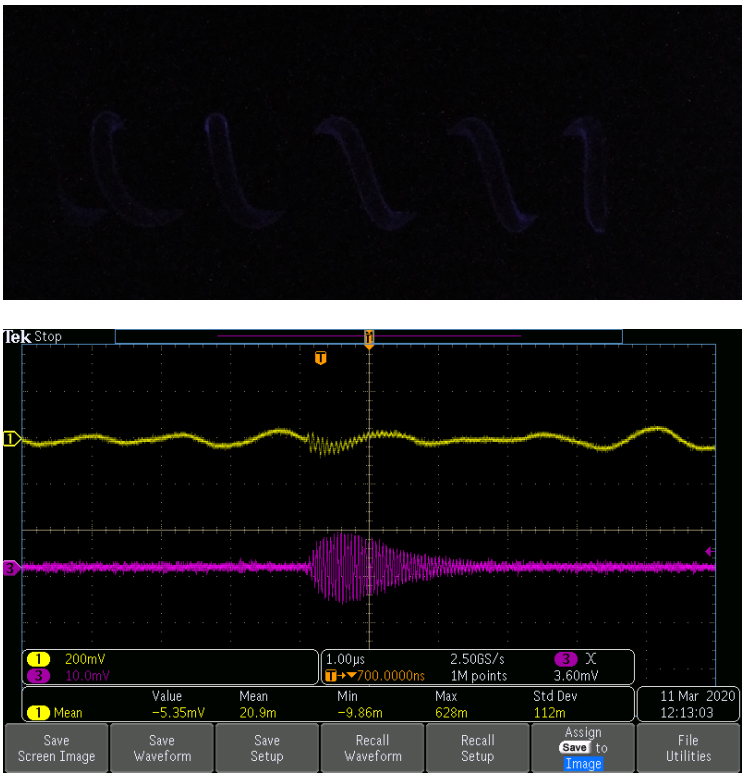

Figure 41: Visual and radio-frequency/electrical detection under DC current.

4.3.3 S2: Negative direct current

The results belonging to negative direct current for the aeronautical wire are represented in figure 42 with their corresponding values that are listed in table 8.

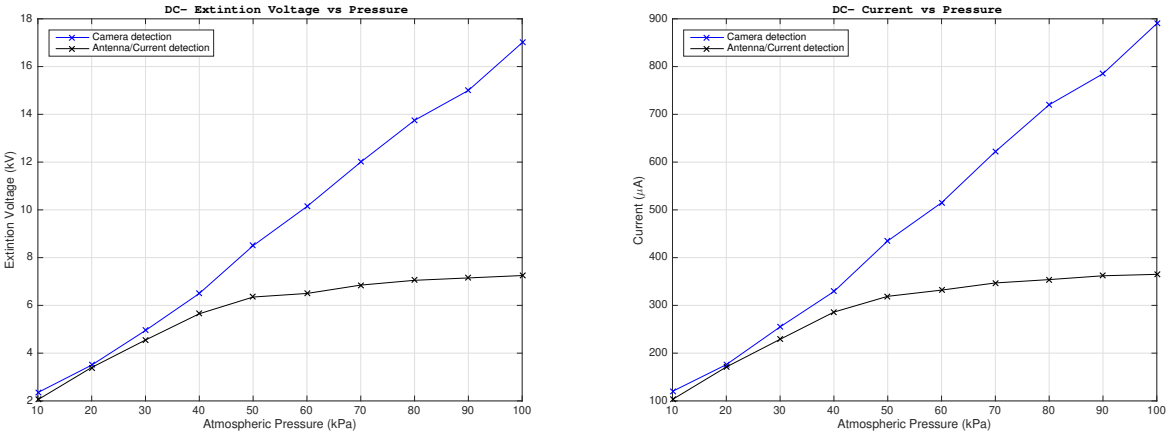

Figure 42: M22759/34 sample test without defect under negative direct current.

	Visual Detection		Antenna Detection	
Pressure (kPa)	**CEV (kV)**	**Current (μA)**	**CEV (kV)**	**Current (μA)**
10	2.35	120	2.05	103
20	3.50	176	3.40	171
30	4.95	255	4.55	229
40	6.50	329	5.65	286
50	8.50	435	6.35	319
60	10.14	515	6.50	332
70	12.00	622	6.85	347
80	13.75	720	7.05	354
90	**15.00**	**785**	7.15	362
100	**17.00**	**890**	7.25	365

Table 8: Sample 2: DC- results for visual and antenna detection.

Surprisingly, the behavior between sample 1 and sample 2 for the case of negative direct current is totally different, unlike the previous two cases for AC and positive DC which is almost the same and the only thing that varies are the values that increase by the cable insulation. In the graphs, it can be seen how there is a great difference between the two values in the same pressure and how high the insulator can withstand partial discharges when subjected to negative DC. As in the case of positive DC, the partial discharges appear long before they do it visually and when they do, the electric arc is created directly so it is not perceived visually. At some point in the tests, some of the corona effect could be identified in the cable, however, since it is a dimmer light than that produced by positive AC or DC, it is not fully visible. Finally, by carrying out tests for the pressure of 90 kPa and 100kPa, the extinction voltage exceeds the voltage that can be generated by the electrical source, so these last two values have been estimated according to the trend of the line. With this it can be concluded that, in effect, the partial discharges appear slower and at a higher voltage in DC- than in AC and DC +.

4.4 Sample 3: Cable coiled around a copper tube with defect on insulating coat

To finish the study of the corona effect in wires, we wanted to use a common setup in the study of partial discharges where a small cut is made in the insulating part. In addition, in this section the test will be carried out in alternating current since it is generally the most restrictive and affects more forcefully compared to direct current. In figure 43 it is seen the graphs obtained in the tests with their corresponding values listed in table 9.

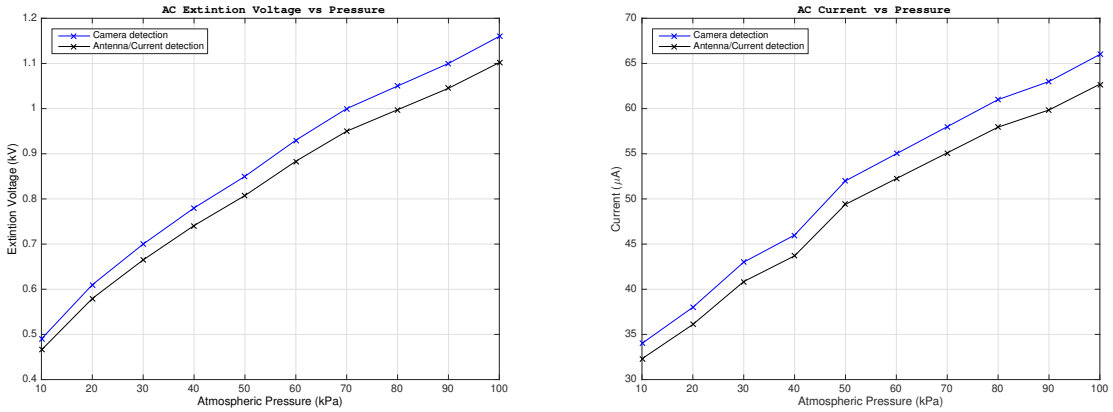

Figure 43: Sample 3 test under alternating current.

	Visual Detection		Antenna Detection	
Pressure (kPa)	**CEV (kV-AC)**	**Current (μA)**	**CEV (kV-AC)**	**Current (μA)**
10	0.49	34	0.47	32
20	0.61	38	0.58	36
30	0.70	43	0.67	41
40	0.78	46	0.74	44
50	0.85	52	0.81	49
60	0.93	55	0.88	52
70	1.00	58	0.95	55
80	1.05	61	1.00	58
90	1.10	63	1.05	60
100	1.16	66	1.10	63

Table 9: Sample 3: AC results for visual and antenna detection.

From the graphs it can be seen that the behavior is the same as in the previous cases where the extinction voltage with respect to the pressure maintains a linear trend. Although there is the presence of a defect in the insulator part, the values are similar to the other setups previously studied, the only thing that could be differentiated from the others is that the transition of the corona effect does not have a high interval to increase the intensity of brightness but at the same time there is a high risk of arcing. Figure 44 shows that although the corona effect is more visible in AC, there is not much intensity in the glow and that the electric arc appears earlier than in the other cases.

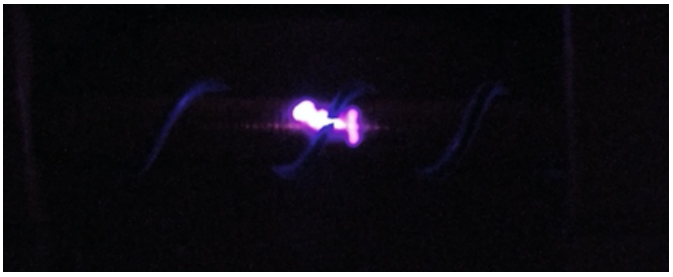

Figure 44: Visual detection on sample 3.

4.5 Polarity effect: Comparative Positive and Negative DC

One of the characteristics to highlight of the corona effect under direct current is that the magnitude of the electric field to create the appearance of the corona depends on the space charge available, however, this accumulated space charge can be neglected at the time of inception and only consider the shape of the sample.

Regarding to negative polarity it is known that corona produces thicker plasma regions and more number of electrons than those produced in positive coronas. The plasma region extends beyond the ionization region because electrons are repelled from the negative electrode and conducted to ground, thus increasing the corona current. Under positive polarity, the heavier and slower positive ions are also repelled from the positive electrode, and conducted to ground at a lower speed, whereas the electrons are involved in the discharge activity in the high field region around the positive electrode. Positive corona pulses exhibit higher amplitudes than negative pulses, although the last ones are more frequent. This explains why the positive polarity corona current is lower than the negative one. It is also known that negative corona exhibits more variability than positive corona because of the presence of discharge spots in variable locations [6].

The polarity effect is a phenomenon that affects the dielectric behavior of relatively long air gaps such as rod-plane, spike-plane, or sphere-plane configurations with the plane grounded, when changing the polarity of the applied dc voltage. Due to this effect, the corona current, corona losses, and breakdown voltage are higher under negative DC polarity compared to positive DC polarity [6]. This conclusion can be valid when performing tests on sample 3 (spike-plane method), because the features are the same such as distance to the spike or electrode from ground. But when performing tests to samples such as sample 2 or sample 3, apart from hardly seeing the corona, the inception voltage was close to the spark breakdown.

4.6 Sample 4: Arc detection at 0.5 mm distance among electrodes

In these last two tests, it is wanted to find out the breakdown voltage according to the distance between the two electrodes that are at different potential, at one end it is connected to ground and the other connected to high voltage, to get a safety range when the first partial discharges begin to be detected until this undesired rise of voltage and current is created to avoid failures in the systems and devices carried by the aircraft. In figure 45 it is possible to see the graphs obtained in the tests with their corresponding values listed in table 10 for a distance of 0.5 mm between electrodes.

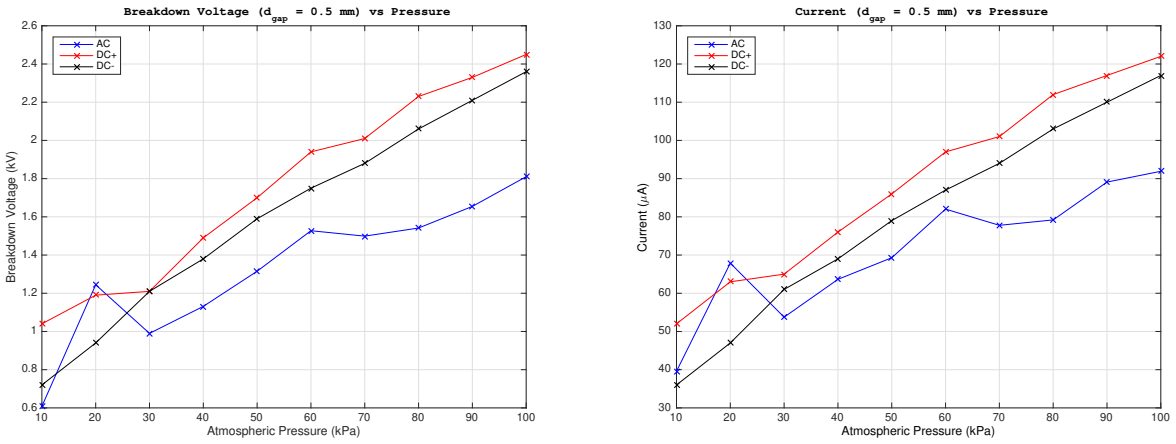

Figure 45: Breakdown voltage and current for a gap of $d = 0.5$ mm.

	AC		DC+		DC-	
P (kPa)	**CEV (kV)**	(μA)	**CEV (kV)**	(μA)	**CEV (kV)**	(μA)
10	0.61	40	1.04	52	0.72	96
20	1.24	68	1.19	63	0.94	146
30	0.99	54	1.21	65	1.21	179
40	1.13	64	1.49	76	1.38	216
50	1.32	69	1.70	86	1.59	239
60	1.53	82	1.94	97	1.75	273
70	1.50	77	2.01	101	1.88	305
80	1.54	80	2.23	112	2.06	332
90	1.65	89	2.33	117	2.21	360
100	1.81	92	2.45	122	2.36	385

Table 10: Sample 4: AC, DC+ and DC- results for arcing detection (d = 0.5 mm).

To better understand the behavior and see the differences between the different types of currents, the data from the three tests have been placed on the same graph. Knowing that 0.5 mm is a relatively short distance, for a pressure as low as 10 kPa where the electric arc is prone to be created, we see that the maximum voltage that can be reached is 0.61 kV for AC, in DC + it resists up to 1.04 kV and at DC- 0.72 kV. When it was carried out the tests of our aeronautical cable, we see in the table 6 that in AC we obtained a value of 0.47 kV-AC that if we passed it to a peak value it would be about 0.66 kV and thus being able to obtain a margin of 50V until the electric arc is created. Even if the cable has an insulator, the arc could appear at a higher voltage. It can also be observed that of the three lines, the most prone to failure before is the one subjected to alternating current. It should be noted that these results could vary according to factors such as the temperature and humidity of the vacuum chamber, so a peak can be observed in the line of the results for alternating current at a pressure of 20 kPa.

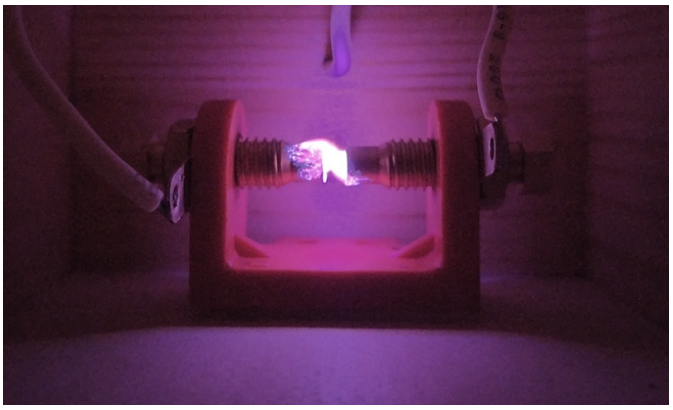

Figure 46: Arcing visual detection for a gap of $d = 0.5$ mm.

4.7 Sample 5: Arc detection at 3 mm distance among electrodes

Now changing the electrode distance to 3 mm, it is possible to see in table 11 how the breakdown voltages have increased without having changed another parameter. In the previous case we had that for AC at 10 kPa the voltage at which the arc appeared was 0.61 kV, however, now it has increased to 2.05 kV, also for 100 kPa the breakdown voltage was 1.81 kV and now it is 7.90 kV. Another interesting fact regarding the previous section is that from the three types of currents now the most likely to fail before is the DC positive, while at 0.5 mm it is AC.

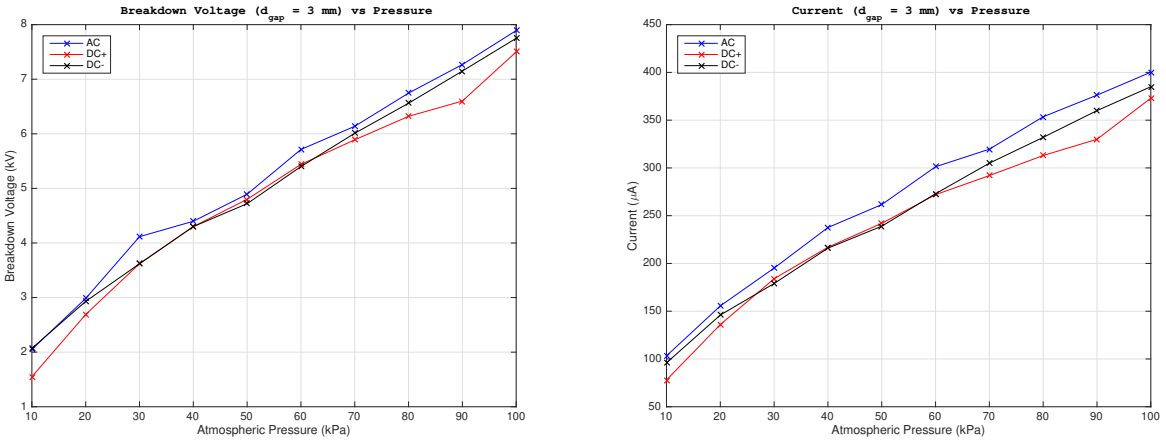

Figure 47: Breakdown voltage and current for a gap of $d = 3$ mm.

	AC		DC+		DC-	
P (kPa)	**CEV (kV)**	(μA)	**CEV (kV)**	(μA)	**CEV (kV)**	(μA)
10	2.05	103	1.55	78	2.07	36
20	2.98	156	2.69	136	2.93	47
30	4.12	195	3.62	184	3.62	61
40	4.40	238	4.30	217	4.30	69
50	4.90	262	4.80	242	4.72	79
60	5.71	301	5.44	272	5.40	87
70	6.14	320	5.89	292	6.01	94
80	6.75	354	6.32	313	6.56	103
90	7.27	376	6.60	330	7.15	110
100	7.90	400	7.50	373	7.75	117

Table 11: Sample 5: AC, DC+ and DC- results for arcing detection (d = 3 mm).

It is important that when performing the tests for any of the previous samples, it is verified that the environmental conditions such as temperature, humidity and pressure are the same in all cases so that there is a high percentage of credibility in the results. For the electric arc tests, it has not been proceeded to analyze directly in the circuit or with the antenna since the electric arc happens spontaneously and it is difficult to capture this voltage rise with the oscilloscope while taking the voltage and current data from the multimeter, so that the results are also an estimate of the data obtained from different tests and that they do not differ much from those presented in this work.

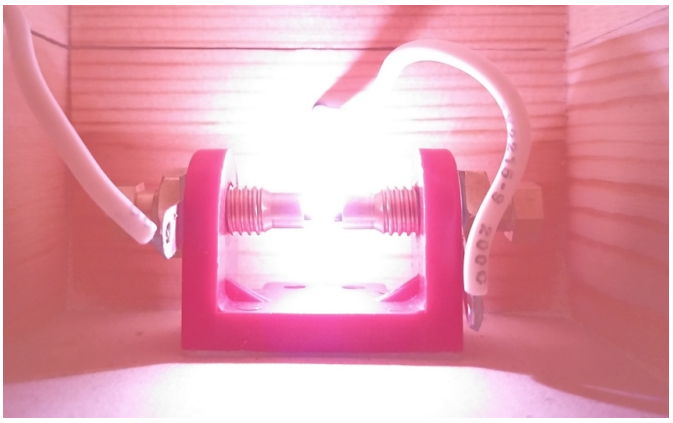

Figure 48: Arcing visual detection for a gap of $d = 3$ mm.

5 Conclusions

After having carried out the first tests of the project, experimentally, it has been detected that the voltage-pressure curve has a linear trend. The theory that pressure does affect the appearance of partial discharges is confirmed since, at very low pressures and depending on the insulating material, the inception voltage is lower.

It has also been detected that the behavior of the insulator in the face of the different types of current, that is, alternating and direct, is not the same. As regards visual detection, the corona effect is seen earlier under alternating current than in direct current, as can be seen in the graphs in the results section, the inception voltage in direct current for both polarities is slightly higher than in alternating current. In addition, ultraviolet light due to ionization of the air around the cable is dimmer when the sample is subjected to direct current than alternating. For this reason, the corona effect in alternating current is more visible in the images. It could be that the exposure time to take the photo is not long enough to capture a large number of photons and so the corona is more visible. A camera would be needed that could have more exposure time than the used mobile, whose maximum time is 32 seconds.

During the process of taking the results, thanks to the consulted literature, the setup applied to obtain the test data, it has improved, going from having only one detection method to three methods, allowing the identification of partial discharges with greater precision since it was discovered that the method by radio-frequency and electrical, partial discharges are detected earlier than by visual detection. It can be seen that, in alternating current, the curve corresponding to visual detection, although it is subsequently detected, is very close to the curve by detection using antenna. However, in direct current, the two curves are slightly separated, meaning that partial discharges may be present but become visible at a higher voltage.

On the other hand, the tests carried out to detect the voltage at which the electric arc jumps, the trend is also linear for the two types of current. Although, as it has been observed in Figure 45, at some point it is not exactly linear in behavior since factors such as the state of the cable or the electrodes, environmental conditions within the vacuum chamber such as the amount of ozone generated in the previous test, temperature and humidity can alter the breaking voltage. Two tests were carried out at different distances and we can corroborate that the rupture voltage also depends on the distance, as has been demonstrated with pressure. The less distance to the other electrode, the lower the voltage required for arcing. It is also important to emphasize that when tests were carried out to study the corona effect by visual detection in direct current, the voltage at which the corona became visible was very close to arcing.

From the results and the study carried out in this project, the most restrictive type of current or the one that can most favor the appearance of partial discharges in the wiring previously, is that of alternating current. Although there are cables for different voltage levels and they are prepared to work at the marked tension, it should be borne in mind that the cables suffer damage and are subjected to all types of cycles such as vibrations, heating or are contamination with chemicals that may favor early appearance of partial discharges. Therefore, it is advisable to take this phenomenon into account and periodically review the wiring in aircraft in order to verify that they are in the necessary conditions to operate and ensure the correct operation of the electrical system.

References

[1] Lucjan Setlak, Emil Ruda *Review, Analysis and Simulation of Advanced Technology Solutions of Selected Components in Power Electronics Systems (PES) of More Electric Aircraft.* World Academy of Science, Engineering and Technology. International Journal of Computer and Systems Engineering Vol: 9, No: 10, 2015.

[2] ZVEI - German Electrical and Electronic Manufacturers' Association. *Measurement and diagnosis of partial discharges in low voltage applications ≤ 1000 volts* . Electrical Winding Insulation Systems Division, Germany, January 2017.

[3] Benjamin Cella. *On-line partial discharges detection in conversion systems used in aeronautics.* Electric power. Université Paul Sabatier - Toulouse III, 2015. English. NNT : 2015TOU30337. tel-01416528.

[4] Joseph Kurek, Robert Bernstein , Mike Etheridge, Gary LaSalle, Roy McMahon, Jim Meiner, Noel Turner, Michael Walz, and Cesar Gomez. *Aircraft wiring degradation study.* Washington D.C, U.S. Dept. of Transportation, Federal Aviation Administration, 2008.

[5] Xiong, Han. *Detection and Pattern Recognition of Partial Discharge in Electric Machine Coils with Pulsed Voltage Excitation.* 2019.

[6] Jordi Riba, Andrea Morosini, Francesca Capelli. *Comparative study of AC and positive and negative DC visual corona for sphere-plane gaps in atmospheric air.* Article in Energies, October 2018.

[7] Roberto Sosa, Elise Arnaud, Etienne Mémin, Guillermo Artana. *Study of the Flow Induced by a Sliding Discharge.* IEEE Transactions on Dielectrics and Electrical Insulation, Institute of Electrical and Electronics Engineers, 2009, 16 (2), pp.305-311. ff10.1109/TDEI.2009.4815157ff. ffinria-00377307f.

[8] Pezhman Zolfaghari , Hamid Reza Khaledian, Nasrin Aliasgharlou, Sirous Khorram, Afzal Karimi, Alireza Khataee. *Facile surface modification of immobilized rutile nanoparticles by non-thermal glow discharge plasma: Effect of treatment gases on photocatalytic process.* June 2019.

[9] Electric discharge in gases. *Wikipedia*. Last seen: 24/03/2020. Available online: https://en.wikipedia.org/wiki/Electric_discharge_in_gases

[10] Mustafa Cavcar. *The International Standard Atmosphere*. Anadolu University, 26470, Eskisehir, Turkey.

[11] Jordi Riba, Álvaro Gómez-Pau, Manuel Moreno-Eguilaz. *Experimental Study of Visual Corona under Aeronautic Pressure Conditions Using Low-Cost Imaging Sensors*. Article in Sensors, January 2020.

[12] AC 21-99. *Aircraft Wiring and Bonding Sect 2 Chap 17*.

[13] ASTM D2303-13, Standard Test Methods for Liquid-Contaminant, Inclined-Plane Tracking and Erosion of Insulating Materials, ASTM International, West Conshohocken, PA, 2013, www.astm.org.

[14] IEC 60587 , Electrical insulating materials used under severe ambient conditions - Test methods for evaluating resistance to tracking and erosion, Third edition 2007-05.

[15] ASTM D2132-19, Standard Test Method for Dust-and-Fog Tracking and Erosion Resistance of Electrical Insulating Materials, ASTM International, West Conshohocken, PA, 2019, www.astm.org

[16] ASTM D3638-12, Standard Test Method for Comparative Tracking Index of Electrical Insulating Materials, ASTM International, West Conshohocken, PA, 2012, www.astm.org

[17] Thomas J. Stueber, Ahmad Hammoud, David McCall. *Comparison of arc tracking tests in various aerospace environments*. NASA Lewis Research Center , 1996.

[18] Cahill, Patricia. *An evaluation of the flammability of aircraft wiring*. Washington D.C, U.S. Dept. of Transportation, Federal Aviation Administration, 2004.

[19] F. Dricot, and H. J. Reher. *Survey of Arc Tracking on Aerospace Cables and Wires*. ERNO Raumfahrttechnik GmbH, Bremen, Germany, 1994.

[20] AC. 251701, Certification of Electrical Wiring. *Aircraft Electrical Wiring Interconnect System (EWIS) Best Practices*. Federal Aviation Administration, 2008.

[21] Paterson, Alex. *Aircraft electrical wires types.* An aviation safety article, 2012. Available online: `http://www.vision.net.au/~apaterson/aviation/wire_types.htm`

[22] V. Degardin, L. Kone, P. Laly, M. Lienard, F. Valensi. *Measurement and analysis of arc tracking characteristics in the high frequency band.* IEMN/TELICE; University of Lille, INP/Laplace; University Paul Sabatier, 2016.

[23] Hanson, Josef and Koenig, Dieter *Fault Arcs Effects in Cable Bundles for Space Applications in Vacuum.* Darmstadt University of Technology, High Voltage Laboratory, Darmstadt, Germany, 1997.

[24] *"Standard test method for thermal endurance of film-insulated round magnet wire", D2307-05.* ASTM International, West Conshohocken, PA, 2005, www.astm.org

[25] H. El Bayda, F. Valensi, M. Masquère and A. Gleizes. *Energy Losses from an Arc Tracking in Aeronautic Cables in DC Circuits.* Université de Toulouse, UPS, INPT ; LAPLACE (Laboratoire Plasma et Conversion d'Energie), 2013.

[26] T André, F Valensi, P Teulet, Y Cressault, T Zink and R Caussé *Arc tracking energy balance for copper and aluminum aeronautic cables.* Université de Toulouse UPS, INPT ; LAPLACE. Airbus Operations S.A.S, 2017.

[27] Rui Rui and Ian Cotton. *Impact of Low Pressure Aerospace Environment on Machine Winding Insulation.* School of Electrical Electronic Engineering. University of Manchester, 2010.

[28] Nitric acid Toxicological Overview, Public Health England, December 2017.

[29] Athanasios C. Mermigkas, David Clark, and A. Manu Haddad. *Investigation of high altitude/tropospheric correction factors for electric aircraft applications.* AHIVE Research Centre, Cardiff University, 2019.

[30] British standard 62068, "Electrical insulation systems — Electrical stresses produced by repetitive impulses — Part 1: General method of evaluation of electrical endurance".

[31] ASTM D1868 – 07, 'Standard Test Method for Detection and Measurement of Partial Discharge (Corona) Pulses in Evaluation of Insulation Systems', 2007.

Appendix

The code that has been used to obtain the data remotely from the mobile phone, has been programmed according to the command language called Bash.

```
#!/bin/bash

# catch de errores a funcion printerr
trap 'printerr $LINENO' ERR

# PHONEIP="10.192.196.100"
# PHONEIP="192.168.0.28"
PHONEIP="192.168.1.34"
FOLDER="2020_03_11"
# FOLDER=$(date '+%Y_%m_%d')
NWAIT=33

# imagen de referencia para superponer
# REFIMAGE="RES_20200213_115118_1__ac_electrodes_3mm_90kPa_x.xxkV.jpg"

RES=15
TOL=5

INFO="dc_pos_M22759_100kPa_11.65kV"

# ============================================================

# merge de imagenes
# convert RES_20200211_144025__ac_electrodes_100kPa_0.00kV.jpg ...
    RES_20200211_145731__ac_electrodes_100kPa_7.85kV.jpg -gravity center ...
    -define compose:args=80 -compose blend -composite resu.jpg

# adb kill-server && adb start-server

# adb devices
# adb tcpip 5555
# adb connect $PHONEIP:5555

# sshpass -p corona123 ssh -p 2222 $PHONEIP
```

```
33 # cd /data/data/com.arachnoid.sshelper/files/home/SDCard/DCIM/Camera
34
35 TAP=${1-""}
36
37 function printerr {
38     echo "Hi ha hagut un error! ($1)"
39     echo "Acabat"
40     exit 1
41 }
42
43 # ============================================================
44
45 figlet "Taking photo"
46
47 if [ $TAP ]; then
48     echo "Fent tap..."
49     adb shell 'input tap 540 1170'
50     sleep 1
51 fi
52
53 adb shell 'input keyevent KEYCODE_CAMERA'
54
55 N=$NWAIT
56
57 while [ $N -gt 0 ]; do
58     echo -n "$N "
59     sleep 1
60     N=$(($N-1))
61 done
62
63 echo "0, Foto feta!"
64
65 # ============================================================
66
67 figlet "Checking time"
68
69 cat << EOF | sshpass -p corona123 ssh -p 2222 $PHONEIP | tee delme.txt
70 cd /data/data/com.arachnoid.sshelper/files/home/SDCard/DCIM/Camera
71 ls -tr *.jpg | tail -n 1
72 EOF
73
```

```
74  DELFILE=$(tail -n 1 delme.txt)
75  HIMG=10#${DELFILE:13:2}
76  MIMG=10#${DELFILE:15:2}
77  SIMG=10#${DELFILE:17:2}
78  SECIMG=$(($HIMG*3600+$MIMG*60+$SIMG))
79
80  NOW=$(date +%H%M%S)
81  HNOW=10#${NOW:0:2}
82  MNOW=10#${NOW:2:2}
83  SNOW=10#${NOW:4:2}
84  SECNOW=$(($HNOW*3600+$MNOW*60+$SNOW))
85
86  DELTA=$(($SECNOW-$SECIMG))
87
88  echo "$DELTA seconds!"
89
90  if [ $DELTA -gt $((2*$NWAIT)) ]; then
91      echo "Es posible que no se haya hecho foto"
92      echo "Enter para seguir o Ctrl+C para cancelar"
93      read DUMMY
94  fi
95
96  # ============================================================
97
98  figlet "Renaming"
99
100 cat << EOF | sshpass -p corona123 ssh -p 2222 $PHONEIP | tee name.txt
101 cd /data/data/com.arachnoid.sshelper/files/home/SDCard/DCIM/Camera
102 FILE=\$(ls -tr *.jpg | tail -n 1)
103 FILENEW="\${FILE%.jpg}__$INFO.jpg"
104 mv \$FILE \$FILENEW
105 echo \$FILENEW
106 EOF
107
108 # ============================================================
109
110 figlet "Copying"
111
112 IMGFILE=$(tail -n 1 name.txt)
113
114 sshpass -p corona123 rsync -avP -e "ssh -p 2222" ...
```

```
    $PHONEIP:/data/data/com.arachnoid.sshelper/files/home/SDCard/DCIM/Camera/$IMGFILE ...
    $FOLDER/
115
116 # ============================================================
117
118 figlet "Processing"
119
120 # rotacion correcta
121 echo "Rotating..."
122 jhead -autorot $FOLDER/$IMGFILE
123
124 # reescalado
125 echo "Scaling..."
126
127 RESFILE=RES${IMGFILE#IMG}
128 convert $FOLDER/$IMGFILE -resize ${RES}% $FOLDER/$RESFILE
129
130 # contraste
131 echo "Contrast..."
132
133 ZZZFILE=ZZZ${IMGFILE#IMG}
134 convert $FOLDER/$RESFILE -fuzz ${TOL}% -fill white -opaque black ...
    $FOLDER/$ZZZFILE
135
136 # merging
137 echo "Merging..."
138
139 MERFILE=MER${IMGFILE#IMG}
140
141 #if [ ! -e $FOLDER/$MERFILE ]; then
142     #convert $FOLDER/$REFIMAGE $FOLDER/$RESFILE -gravity center -define ...
        compose:args=80 -compose blend -composite $FOLDER/$MERFILE
143 #fi
144
145 # histograma
146 echo "Histogram..."
147
148 DATFILE=$IMGFILE
149 DATFILE=DAT${DATFILE#IMG}
150 DATFILE=${DATFILE%.jpg}.dat
151
```

```
152 HISFILE=$IMGFILE
153 HISFILE=HIS${HISFILE#IMG}
154 HISFILE=${HISFILE%.jpg}.png
155
156 X=$(($TOL*256/100))
157
158 convert $FOLDER/$RESFILE -format %c histogram:info:- |
159     sed 's/[,():]/ /g' |
160     awk -f process.awk > $FOLDER/$DATFILE
161
162 gnuplot << EOF
163 set terminal png
164 set output "$FOLDER/$HISFILE"
165 set xrange [0:255]
166 # set logscale x
167 set xlabel "Color intensity bin"
168 set ylabel "Number of pixels"
169 plot \
170 "$FOLDER/$DATFILE" u 1 w l lc "red" title "Red",\
171 "$FOLDER/$DATFILE" u 2 w l lc "green" title "Green",\
172 "$FOLDER/$DATFILE" u 3 w l lc "blue" title "Blue"
173 set arrow from $X,graph 0 to $X,graph 1 nohead lc "gray"
174 replot
175 EOF
176
177 # ============================================================
178
179 figlet "Visualizing"
180
181 #feh $FOLDER/{$RESFILE,$MERFILE,$ZZZFILE,$HISFILE}
```